

**Application of the Biaxial Iosipescu Test Fixture for the Mechanical
Characterization of Unidirectional Composites**

Maharajapuram.V. Balakrishnan
M.E. (Metallurgy)
Indian Institute of Science
Bangalore, India, 1991

A dissertation submitted to the faculty of the
Oregon Graduate Institute of Science & Technology
in partial fulfillment of the
requirements for the degree
Master of Science
in
Materials Science and Engineering

September, 1995

The dissertation “Application of the Biaxial Iosipescu Test Fixture for the Mechanical Characterization of Unidirectional Composites” by Maharajapuram.V. Balakrishnan has been examined and approved by the following Examination Committee.

Dr. M.S. Kumosa
Thesis Research advisor
Associate Professor
Dept. of Materials Science and Engineering

Dr. D.G. Atteridge
Professor
Dept. of Materials Science and Engineering

Dr. J. Devletian
Professor
Dept. of Materials Science and Engineering

To “Amma” and “Appa”

Acknowledgments

I wish to thank my advisor Dr. Maciej Kumosa for his support and assistance to accomplish this work.

Thanks to my thesis committee- Drs. D.G. Atteridge, Dr. J. Devletian for their critical reading my dissertation. I also would like to thank the staff members of the Department of Materials Science and Engineering - Mr. Glen Ramirez, Mr. Ken Burns, Mr. Jack McCarthy and Ms. Kristen Terry for their various help.

I thank my friends Venky, Srikanth, Don, Priya, Sai, Anurag, Shialiang Ding and Partha for their help, company and making my stay a pleasurable affair.

Funding for this project came from the National Science Foundation and Electric Power Research Institute.

Table of Contents

	Page
DEDICATION	iii
ACKNOWLEDGEMENTS	iv
TABLE OF CONTENTS	v
LIST OF TABLES	vii
LIST OF FIGURES	viii
ABSTRACT	xi
Chapter 1 Introduction	1
Chapter 2 Background	4
2.1: Shear Testing of Composites	4
2.1.1: Tube Torsion Test	5
2.1.2: Off-axis Test	5
2.1.3: Iosipescu Shear Test	6
2.2: Biaxial Testing	10
2.3: Fatigue Testing	13
2.3.1: Biaxial Testing of Composites under Cyclic Loading	13
2.4: Summary:	15
Chapter 3 Experimental Details	24
3.1: Biaxial Iosipescu Test Fixture	24
3.2: Test Methodology	25
3.3: Experiments	27
3.3.1: Test Materials	27
3.3.2: Mechanical Tests	27

Chapter 4 Biaxial Testing of a SiC/Ti Metal Matrix Composite	31
4.1: Introduction	31
4.2: Material Tested	31
4.2.1: Static Testing	32
4.3: Finite Element Analysis	33
4.4: Biaxial Fatigue Testing	34
4.5: Results and Discussion	36
4.6: Limitations	37
4.7: Conclusions	37
Chapter 5 Biaxial Testing of Glass Reinforced Polymer (GRP) Matrix Composites . .	51
5.1: Introduction	51
5.2: Material Tested	51
5.2.1: Experimental Procedure	52
5.3: Results	52
5.4: Conclusions	54
Chapter 6 Biaxial Testing of Unidirectional Carbon/Epoxy Composite	61
6.1: Introduction	61
6.2: Experimental Procedure	61
6.3: Experimental Results	63
6.3.1: Mechanical Test Results	63
6.3.2: Fractography	64
6.4: Discussion	66
6.5: Conclusions	70
Chapter 7 Conclusions	87
REFERENCES	89

List of Tables

	Page
Table 2-1: Comparative Study of the Various Shear Test Methods [31]	16
Table 4-1: Material properties of the Matrix and Fiber	38
Table 4-2: Mechanical properties used for the FEM Analysis	38
Table 4-3: Biaxial Fatigue Test Results for Al-6061 T-6 alloy.	39
Table 4-4: Fatigue Test results for the SiC/Ti metal matrix composite.	39
Table 6-1: Shear Test Results (using Biaxial Iosipescu Test Fixture)	71
Table 6-2: Shear Test Results (using Idaho Test Fixture)	71
Table 6-3: Off Axis Test Results	72
Table 6-4: Biaxial Iosipescu Test Results (with loading angle variation)	73
Table 6-5: Off-axis Iosipescu Test Results	74
Table 6-6: Transverse Tensile Test Results	76

List of Figures

	Page
Figure 2-1: Tube torsion test.	17
Figure 2-2: Off-axis test.	17
Figure 2-3: Iosipescu shear test.	18
Figure 2-4: Force, Moment, and shear diagram for the Iosipescu specimen	19
Figure 2-5: Cruciform specimen	20
Figure 2-6: Arcan specimen	20
Figure 2-7: Loading configuration in the biaxial Iosipescu test fixture	21
Figure 2-8: Biaxial loading configuration of tubular specimens	22
Figure 2-9: Biaxial fatigue failure envelope for Glass/epoxy composite [51].	23
Figure 2-10: Isochronous plots for biaxial fatigue failure representation [52].	23
Figure 3-1: Biaxial Iosipescu test fixture.	28
Figure 3-2: Estimated normal stresses using fiber angle variation.	29
Figure 3-3: Estimated value of the shear stresses using fiber angle variation	29
Figure 3-4: Estimated biaxiality ratios using fiber angle variation.	30
Figure 4-1: Shear stress - strain diagram	40
Figure 4-2: Load-displacement diagram under static loading	40
Figure 4-3: Load-displacement diagram under static loading	41
Figure 4-4: Biaxial failure envelope for the tested SiC/Ti metal matrix composite. ...	41
Figure 4-5: Normal stress distribution along the notch root axis.	42
Figure 4-6: Shear stress distribution along the notch root axis	42
Figure 4-7: Analytical and numerical estimation of average stresses in the specimen	43
Figure 4-8: Optical micrograph of a specimen loaded in fatigue	44

Figure 4-9: Schematic of the failure modes under fatigue	45
Figure 4-10: SEM micrograph of the fracture surface	46
Figure 4-11: SEM micrograph of the fracture surface	47
Figure 4-12: SEM micrograph of the fracture surface	48
Figure 4-13: Lateral view of the split developed under fatigue	49
Figure 4-14: Transverse view of the fatigue fracture surface	50
Figure 5-1: Biaxial Failure loads for E-glass/vinylester system	55
Figure 5-2: Biaxial Failure loads for E-glass/epoxy system	55
Figure 5-3: Biaxial Failure loads for E-glass/polyester system	56
Figure 5-4: Load-displacement plots for dry and wet E-glass/epoxy specimens	56
Figure 5-5: Moisture distribution with time for E-glass/vinylester composite.	57
Figure 5-6: Moisture distribution with time for E-glass/epoxy composite.	57
Figure 5-7: Moisture distribution with time for E-glass/polyester composite.	58
Figure 5-8: Biaxial failure envelope for E-glass/vinylester system	58
Figure 5-9: Biaxial failure envelope for E-glass/epoxy system	59
Figure 5-10: Biaxial failure envelope for E-glass/polyester system	59
Figure 5-11: Biaxial failure envelope for the E-glass/GRP systems (dry conditions). .	60
Figure 6-1: Schematic of the observed failure modes in the various tests.	77
Figure 6-2: Photo-micrograph of the axial splits in the Iosipescu specimens.	78
Figure 6-3: Failure loads for the tested specimens as a function of the loading angle.	79
Figure 6-4: Failure loads for the tested specimens as a function of the fiber angle. ..	79
Figure 6-5: Fracture surface morphology of the Iosipescu specimen.	80
Figure 6-6: Fracture surface morphology of the Iosipescu specimen	81
Figure 6-7: Fracture surface morphology of the off-axis specimen.	82
Figure 6-8: Fracture surface morphology of the Iosipescu specimen.	83
Figure 6-9: Fracture surface morphology of the tested transverse tensile specimen. .	84
Figure 6-10: Shear test results from the employed test methods.	85

Figure 6-11: Comparison of the average shear strengths from the various tests. 85

Figure 6-12: Normal versus shear stress at failure for the biaxial tests performed. . . . 86

ABSTRACT

Application of the Biaxial Iosipescu Test Fixture for the Mechanical Characterization of Unidirectional Composites

Maharajapuram.V. Balakrishnan
Supervising professor: Dr. M. Kumosa

Unidirectional composite (UDCs) materials are being increasingly used in a variety of applications. Their increased usage in the various high performance industries requires a comprehensive mechanical characterization, including property characterization under multiaxial loading conditions. Mechanical characterization of composite materials, and in particular shear testing of composites, pose considerable difficulties and the test methods that are available for multiaxial testing are limited.

A recently developed biaxial Iosipescu test fixture has been used in this study to test UDCs under shear and biaxial loading conditions. This fixture was designed to produce pure shear and biaxial loading conditions under either of static or cyclic loads. In the past, the fixture was only tested under static loading conditions for a limited number of composite systems.

In this research, the biaxial Iosipescu test fixture was used to characterize three different composite systems. Experiments were carried out under shear, and biaxial load-

ings and the intralaminar properties were characterized. In addition, the fixture was used to test the material under biaxial fatigue loading conditions for the first time. An attempt was made to extend the possible range of biaxial loading conditions by orienting the fibers in different directions. It was found from this research that the fixture can successfully be used for intralaminar shear and biaxial property determination of unidirectional composites. By varying the fiber orientation in the specimen, it was shown that the range of biaxial loading conditions can be extended.

Chapter 1

Introduction

Unidirectional composites (UDCs) are either currently being used or are being considered for a variety of applications, from automobile to aerospace industries, owing to their increased specific properties, tailorable nature and high temperature capabilities. Structural application of any such material demands a comprehensive characterization of their mechanical properties. Testing of composites poses considerable difficulty because of their heterogeneous structure and anisotropic nature.

A common use of unidirectional composites is in the form of laminates, comprising several laminae, stacked in different sequences. If all the laminae have the same fiber orientation, then the material can be treated as an unidirectional laminate. Though one can experimentally determine the properties of a laminate, it is necessary that a lamina be evaluated at first for its properties, so that the laminate properties can be derived from the initial properties of the lamina.

The modulus and the strength values can be considered under the static characterization of composites. In principle, a unidirectional composite material can be considered as an orthotropic material with one plane of isotropy perpendicular to the fiber direction. Such a material, called transversely isotropic, would require 5 independent elastic constants to be characterized. If they are modeled as thin plates or shells, then they can be considered as transversely isotropic and plane orthotropic and such a model would need 4 independent elastic constants to be determined, namely, E_{11} , E_{22} , G_{12} , and ν_{12} . Here 11 refers to the fiber direction or axial direction, 22 refers to the transverse direction (prin-

cipal material directions), and 12 will be the in-plane properties. E_{11} , E_{22} , and, ν_{12} can be easily estimated with a simple tension test on specimens with fibers oriented parallel to the loading direction and perpendicular to the loading direction. The measurement of the in-plane shear modulus, G_{12} , requires a pure shear stress state within the gage section of a test specimen, and this makes the shear characterization difficult.

Mechanical characterization would also include strength measurements of the material. Again, for UDCs, the strength values for various fiber orientations needs to be determined. Though, there are simple test methods like off-axis tension tests to measure and model the materials' strength values, it is essential that the composite be evaluated under combined loadings like tension and shear, or compression and shear as the real time use of these materials involves biaxial or triaxial stress states.

What has been discussed, so far, concerns the static property characterization. However, cyclic loading of composites can induce failure and hence the fatigue properties of the material need to be determined. Testing of a laminate, with testing methodologies used for conventional isotropic materials can only evaluate that particular laminate tested. In order to develop a fundamental theory of fatigue failure of a system, one needs to characterize a lamina at first, and develop theories for predicting laminate failure.

A number of test methods have been suggested and used over the last two decades in the shear and biaxial property estimation of unidirectional composites. Most of the presently available test methods warrant a complex testing rig, expensive specimens or produce a questionable stress state in the material. In this research, a recently developed biaxial Iosipescu test fixture has been used for shear and biaxial characterization. The main attractive feature of this test method is that it requires a simple testing rig and can be used for shear and biaxial testing as well. The objective of this research is to explore and extend the use of a biaxial Iosipescu test fixture for the intralaminar property determination of UDCs. The composites were tested for their in-plane shear and biaxial properties under static and/or cyclic loading conditions. Three different composite systems have

been tested in this study; (1) SiC/Ti metal matrix composite, (2) Glass reinforced polymer matrix (GRP) composite, and (3) Carbon fiber reinforced epoxy composite. Chapter 2 gives the background information on the shear and biaxial testing of UDCs. Details on the biaxial Iosipescu test fixture and the conducted experiments are discussed in Chapter 3. In the next three chapters, the experiments and results from the tested composite systems are presented. In Chapter 7 the general conclusions from this study are presented.

Chapter 2

Background

2.1 Shear Testing of Composites

One of the major problems in shear testing of unidirectional materials is the generation of a pure shear stress state in the specimen. Ideally, a shear test method should provide a region of pure, uniform shear stress. This region should be one of maximum shear stress relative to all other regions in the specimen. Further, there should exist a unique relationship between the applied load and the magnitude of the shear stress in the test section. The large number of test methods for shear characterization of composites, proposed during the past twenty years, attests to the difficulties associated with the accurate determination of the shear response of materials. The reason for the problem lies in the inherent nature of the composite material itself. Composite materials are heterogeneous and anisotropic. Their anisotropic nature causes (1) coupling between the normal and shear deformation modes in a coordinate system not aligned with the principal axis, and (2) slow dissipation of Saint Venant's effects caused by the actual boundary conditions [1]. The above two effects often cannot be separated and lead to difficulties in designing specimens with a desirable state of stress in the test section.

Some of the better known shear test methods that are currently in use are: 1) thin walled tube torsion test, 2) 10° off-axis tension test, 3) $[\pm 45^\circ]_s$ laminate test, 4) Iosipescu shear test, 5) rail shear test, 6) cross-beam sandwich test and 7) picture frame test. Tube torsion, Off-axis, and the Iosipescu shear tests are reviewed in this section. A comprehensive review of the shear testing method can be found in Reference [2].

2.1.1 Tube Torsion Test

Torsion testing of tubes[3] (Figure. 2-1) is one of the reliable test procedures for shear property characterization. The special construction of tubular specimens, which is often expensive and troublesome, is a major drawback for this test method. In addition, the prohibitive cost of specimen preparation and the need for highly specialized testing apparatus makes this method less competitive. Furthermore, the different fabrication techniques employed in the manufacturing of tubular and flat composite specimens may result in different response characteristics [4]. Therefore, for applications where flat specimens are required, it is desirable to characterize the shear response of the material on the basis of test methods that employ a flat specimen geometry.

2.1.2 Off-axis Test

Off-axis tests, which employ flat coupons, are widely used for mechanical characterization of unidirectional composites. This method is one of the simplest test methods involving uniaxial loading of flat specimens, with fibers oriented at various angles to the loading axis (Figure 2-2). From the apparent Young's modulus measured for each fiber orientation, the shear modulus can be determined from the equation for the coordinate transformation law for the apparent Young's Modulus (E_θ) for a θ° off-axis specimen [5,6].

$$E_\theta = \left[\frac{\cos^4 \theta}{E_{11}} + \left(\frac{1}{G_{12}} - 2 \frac{\nu_{12}}{E_{11}} \right) \sin^2 \theta \cos^2 \theta + \frac{\sin^4 \theta}{E_{22}} \right]^{-1} \quad (2-1)$$

where θ is the angle between the loading direction and the fiber direction. Since E_{11} , E_{22} , and ν_{12} can readily be measured from simple tension tests of the 0° and 90° specimens, only an additional off-axis specimen is needed to determine G_{12} . The value of G_{12}

is usually determined by choosing a value so that the apparent Young's modulus given by the above equation agrees well with the experimental values. However, this method has a serious limitation: for most off-axis orientations, the applied stresses induce bending and shear in the stress field when conventional clamping methods are used. Moreover, it is difficult to generate a pure shear stress state in the specimen by off-axis loading since there is a strong interaction between normal and shear modes when loaded away from the alignment axis. For tensile loading it is suggested that this problem can be minimized by using rotating grips and by the use of specimens with sufficiently large length/width ratios [7].

The 10° off-axis tensile test is a particular case of the off-axis testing. It was shown by Chamis and Sinclair [8] that the intralaminar shear strain γ_{12} approaches its maximum value at an off-axis angle of $\sim 10^\circ$. The shear stress τ_{12} is the major stress component contributing to failure as determined from a combined stress failure criterion. However, any small misorientation in the fiber orientation and the load alignment can lead to erroneous results. Further, highly orthotropic specimens warrants a large aspect ratio to minimize the end-constraint effects [9].

2.1.3 Iosipescu Shear Test

The Iosipescu shear test has received considerable attention in the past 20 years as a simple shear test procedure for composite materials. The test method was first suggested by Nicolae Iosipescu [10] of Bucharest (Romania), in 1967, for shear strength characterization of metals. The test method achieves a state of pure shear within the test section of a double V-notched specimen by the application counteracting moments produced by two force couples. A schematic of the Iosipescu specimen and the loading configuration is given in Figure. 2-3. The force, shear and moment diagrams are shown in Figure. 2-4. A mechanics of materials analysis indicates a state of constant shear loading in the center section of the test specimen, and this shearing force is equal in magnitude to the applied

load P . The induced moment at the center of the specimen is zero, thereby producing a pure shear stress state at the specimen mid-length. The average shear stress in the specimen is calculated by dividing the external load by the cross sectional area of the specimen mid-section. The notches in the test specimen shift the shear stress distribution from parabolic to uniform. Also, the reduced area along the notches promotes shear failure in the region. Shear test methods employing modified versions of the double edge-notched test specimen have also evolved in the past 20 years. They include 1) Arcan test [11,12], and 2) Asymmetrical four-point bend test [13].

Adams and Walrath [14,15] applied the Iosipescu shear test for testing composite materials and designed a fixture to induce the required loading condition. They have also performed extensive experimental and numerical analysis [16-19] to optimize the specimen geometry as well as the loading fixture. Based on their experimental and numerical investigations they have redesigned the fixture, now called the modified Wyoming fixture. Adams et.al. [17] have also come up with some recommendations for the geometry of the specimen.

Broughton et.al. [20] designed an adaptable in-plane biaxial stress fixture, which was based on the Iosipescu shear test and the Arcan in-plane biaxial test method. From their numerical and experimental investigations, they concluded that the actual shear moduli can successfully be established from the apparent data for the 0° and 90° specimens, by using correction factors to account for the non-uniform shear stress distribution in the specimen. From photoelastic results, they inferred that the force-couple loading condition for finite element analysis best approximates the experimental loading configuration for modelling purposes. Broughton [2,20] used the fixture for shear strength and shear moduli determination of unidirectional carbon fiber reinforced epoxy and PEEK composites. The use of correction factors has also been adopted by Pindera et al [7] in their testing of graphite/epoxy specimens. To avoid the problem of twisting effects in the Wyoming test fixture, Ho et al [21] utilized the average value of the shear strain from the

front and back faces of the specimen. Sullivan [22] suggested that the $\pm 45^\circ$ gages used for strain measurement should read equal and opposite values for a valid shear test. It was shown by Morton et al [23] that this condition need not be met by the 0° specimens because of the load proximity and the low flexural stiffness of the specimen configuration. Morton et al advocate the use of average values from back to back gages to avoid twisting effects. Furthermore, they suggest that a 0° Iosipescu specimen should provide a meaningful value for the shear strength of the material owing to the resistance of the fiber configuration to bending and twisting, together with the uniformity of the shear stress field after initial cracking. Bretz et al [24] have detailed the testing methodology for the Iosipescu shear test and they recommend a 110° notch angle for the test. In the past decade, the Automotive Composites Consortium (ACC) has adopted the Iosipescu shear test for shear characteristics of different materials [25].

Various numerical and experimental studies [16,17,20,26] on the Iosipescu shear test have revealed that the shear stress distribution along the specimen mid-section is not uniform, and correction factors are required to determine the actual shear modulus values from the apparent values. These correction factors are primarily dependent on the orientation of fibers and the specimen orthotropy ratio. It has been suggested [21] that the 90° specimens yield a more accurate shear modulus value than the 0° specimens. Sukumar and Kumosa [27] have analyzed the stress singularities at sharp notches in orthotropic media, through finite element iterative techniques. They concluded that there exists a critical angle below which the singular power vanishes under shear loading. The development of axial splits in 0° Iosipescu specimens have also been numerically analyzed by Sukumar and Kumosa [28]. They have shown that the splits propagate under mixed-mode conditions, and have also proposed mixed mode crack propagation tests using the Iosipescu specimen. In a recent study, Ho et.al. [29] have performed a non-linear numerical analysis of the Iosipescu specimen and have concluded that the non-linear effects due to specimen-

to-fixture contact interactions and specimen geometry on the overall shear response is negligible.

Lee and Munro [30] reviewed the different shear test methods for unidirectional composites in 1986. According to them, the most promising shear test methods include the 10° off-axis tension test, $[\pm 45^\circ]_s$ laminate test, and the Iosipescu shear test. This conclusion was based on a set of eleven criteria ranging from accuracy of stiffness and strength parameter determination, to ease of specimen preparation and testing. However, quite often, the values for the shear parameters measured with these different test methods are significantly different. These discrepancies are caused by incorrect interpretation of the test results in the presence of test section inhomogeneities, and subsequent lack of accurate correlation of the actual stress state in the test section with the apparent or nominal quantities on the assumption of uniformly distributed stress. A combined experimental/analytical methodology was suggested by Pindera [1] to improve the correlation among various shear test results. This methodology essentially involves optimizing the specimen geometry, correctly interpreting the test data in the presence of non uniform deformation fields, and correcting the experimentally introduced errors in testing. A comparative study [31] of the various shear test methods (see Table. 2-1.)

Though the test method has been used for over two decades to measure the shear modulus, attempts to measure the shear strength using this method are restrained [23]. There is a debate in the literature [32], whether the failure strength measured is the actual value, since there is a considerable difference in the apparent strength values from the 0° and 90° specimens. Furthermore, the mode of failure is different in the two specimen configurations; 0° specimens fail by the formation of axial splits initiating at the notch roots and extending away from the inner loading points, while 90° specimens fail along the notch-root axis at a much lower load compared to that of the 0° specimens of the same material. Axial splitting in the 0° specimens occurs with two corresponding load drops in

the load-displacement (or strain) diagram and the specimens, in general, continue to withstand larger loads before the ultimate failure. Failure can be treated as the load for the formation first split, load for the formation of second split, average load for the formation of the axial splits or the maximum load in these tests. In a comparative study, Swanson et.al. [33] have obtained the shear stress corresponding to the first axial split in the Iosipescu test to within 5% with the peak stress for the torsion testing of tubes with the fibers oriented in the hoop direction, in a AS4/3501-6 carbon/epoxy composite system. By considering failure as the average load for the formation of axial splits in the Iosipescu test, Pindera et.al [9] have reported shear strength values to agree within 5% and 7% for aramid-epoxy and graphite/polyimide composites respectively, in comparison to the 10° off-axis tensile test. Morton and Farley's work[23] also suggests that the loads for the formation of the two axial splits in 0° specimens provide an upper-lower bound for the shear strength.

2.2 Biaxial Testing

In most engineering applications, unidirectional fiber composites are subjected to biaxial and triaxial loads. Also the state of stress in each lamina, constituting a laminate, is at least plane; thus, it has three components: σ_{11} in the fiber direction, σ_{22} transverse to the fibers, and τ_{12} in in-plane shear. Hence, it is important to measure mechanical properties and define a failure envelope, under combined stress states. One way to arrive at the failure surface would be to establish the ultimate stress values for single-stress components by experiment, and to construct analytical failure criteria in terms of these values by global consideration. However, experimental determination of the failure surface is needed to verify analytical predictions and requires testing of material under multiaxial loading.

There are two principal methods for testing materials under combined stresses, one utilizing flat specimens, and other using cylindrical specimens, both with various means of applying loads. Flat specimens are easier and cheaper to make than cylindrical specimens, which are in general made by filament winding to a mandrel. The more common forms of reinforcement may also be made into cylinders by wrapping on to a mandrel, but this is likely to result in some form of overlap or discontinuity in the reinforcement.

Off-axis tests have been widely used to produce plane-stress loadings and to evaluate the failure theories [4]. However this test method, as already mentioned, suffers from end-constraint effects, which can produce considerable measurement errors.

Bert et al [34] and Smith and Pascoe [35] used flat cruciform specimens as a means of simultaneously applying two principal stresses (see Figure. 2-5). With this method, it is relatively easy to produce specimens with different fiber orientations relative to the principal axes. However, failure often occurs at corner fillets and the test procedure requires a fairly complex testing rig.

Arcan et al [11] developed a biaxial stress test method, (Figure. 2-6) in which it was possible to produce various combinations of shear and normal stresses. Arcan's test method is similar to the Iosipescu test method, with a variation in the loading configuration. The modified version of the test [12] employs a double V-notched plate specimen glued to a circular Aluminum cutout as shown in Figure.2-6. The earlier version consisted of the entire plate cut in the shape of the present geometry. It should however be mentioned that the significant section of the Arcan specimen is geometrically similar to that of the Iosipescu specimen. This test method has an added variation of loading, in that the loading angle can be varied by rotating the circular cut out with respect to the longitudinal axis (X-axis) of the specimen. The angular range of loading in this test method is limited to $|\alpha| < 45^\circ$, since stress concentrations become appreciable for larger angles. This test method offers a methodology to test plate specimens. However, the main disadvantage [2] is that the failure often occurs at the glue line, specimen-fixture interface,

instead of the gage section. Failure under combined loadings has been generated in the range of $-0.83 < \frac{\sigma_{22}}{\tau_{12}} < 0.83$ using this test method [12] for Scotch-ply reinforced plastic (Type 1002).

The in-plane biaxial Iosipescu test fixture designed by Broughton et.al. [20] is also capable of biaxial loading, apart from pure shear loading. The fixture is based on the Iosipescu shear test and the Arcan in-plane stress method. The loading configuration adopted in the fixture for biaxial loading is shown in Figure. 2-7. The specimens can be rotated from -45° to $+45^\circ$ with respect to the external loading axis. Loading at 0° induces pure shear loading, while for other loading angles a biaxial stress state is induced in the specimen. For biaxial in-plane stress tests the compressive load P is applied at various loading angles α , where α is the angle between P_o and P_α .

This simple test method has successfully been used to derive biaxial failure data for graphite-epoxy [2,20], teak wood [36], glass-polymer [37], and Ti-SiC [38] unidirectional composites. The main disadvantage of this method is that the extent of biaxial loading conditions, that can be simulated is limited, since the loading angle is limited to $\pm 45^\circ$. Further, in practice, there is appreciable sliding of the specimens when loaded at angles larger than 40° . This implies that the specimens can only be loaded with the absolute value of normal stresses less than or equal to shear stress ($|\sigma_{yy}| \leq |\tau_{xy}|$). Therefore, additional tests need be performed under transverse tensile or compressive loading conditions to obtain a complete failure envelope.

Biaxial testing can also be performed by testing thin walled cylinders, under axial (tension or compression), torsional (shear), and pressure (internal or external pressure) loading [4]. The loading configuration for this type of testing is shown in Fig. 2-8. This is definitely a versatile testing since it is possible to apply any desired biaxial state of stress with or without proportional loading. However making test specimens is often expensive

and the test rig is complicated

2.3 Fatigue Testing

Composite materials exhibit complex failure mechanisms under fatigue loading because of their inherent heterogeneity and the anisotropic characteristics of their strength and stiffness [39,40]. Fatigue in composites consists of fiber breakage, matrix cracking, crazing, yielding, debonding, delamination and void formation. The most important difference between fatigue in composite materials and fatigue in homogeneous materials is that fatigue in composite materials does not, in general, consist of a single through-crack which can be detected, monitored, and described by linear elastic fracture mechanics to predict the propagation rate and, therefore, the number of cycles to failure. Despite the differences, fatigue in composites has been studied with the approaches adopted for homogeneous materials. The most common type of investigation is to subject the material under cyclic loading and measure the number of cycles to failure, under a particular stress ratio. The results of such a test are the S-N diagrams. There are several references [41-49] in the literature regarding the fatigue behavior and damage development in composites.

2.3.1 Biaxial Testing of Composites under Cyclic Loading

In the published literature there are relatively very few references on biaxial fatigue tests. The testing systems are much more limited for fatigue testing and all are extensions of the rigs used for biaxial static testing. Here again, one can classify the test rigs in terms of the specimen configuration they use, whether flat or tubular specimens. A biaxial stress state has three components, σ_{xx} , σ_{yy} , and τ_{xy} . In a biaxial test, any two of these components can be independently varied and the rigs that employ flat specimens

usually apply independent normal stresses. Normal and shear stresses are independently varied in rigs employing tubular specimens. Bert et al. [34] and Smith and Pascoe [35] used flat cruciform specimens for fatigue testing in a servohydraulic rig with the applied loads varied by actuators. The specimen geometry for a cruciform specimen is shown in Figure. 2-5. However, with this specimen, stress and strain measurements are difficult, and sometimes it is not possible to prevent failures from initiating at corner fillets [50].

A variety of methods have been used for applying biaxial stresses to cylinders [50] such as (a) internal pressure and axial load, (b) external pressure and axial load, (c) torsion and axial load, and (d) combinations of all three by means of torsion, pressure and axial load. The specimen geometry and the possible loading configuration for this kind of specimen is shown in Figure. 2-8. The cylinder is the most versatile specimen since it is possible to apply any desired biaxial stress state. For cylindrical specimens there are a number of requirements which must be met in order to have confidence in the test results. The cylinder may be treated as being thin-walled provided the stresses are reasonably uniform in the gage section. The length must be sufficient to overcome the end effects and yet prevent buckling under compressive loads. The specimen must be stable under internal pressure or torsion. The ends of the specimen must be reinforced in order to attach grips and prevent end failures. Inhomogeneities due to fabrication and joining techniques can induce bending strains as large as the primary strains due to pressure. The result of biaxial fatigue tests is a failure surface, as shown in Figure. 2-9. for glass/epoxy composites [51]. The results of a biaxial fatigue test can also be plotted as a family of curves, called isochronous plots [52], envelope of biaxial failure stress values for a constant life, N (see Figure. 2-10). The static failure criterion is a special case corresponding to $N=0$. At the other extreme, there are stress states of such low amplitudes that fatigue failure does not occur. This defines the fatigue (or endurance) limit region in Figure. 2-10.

2.4 Summary:

The Iosipescu shear test has been widely accepted as a simple and cost effective test method for shear property characterization. However, extension of the method for biaxial failure envelope generation is limited. Furthermore, there has been no published work in the literature for adopting the test method for cyclic loading. So far the biaxial characterization under static and cyclic loading conditions have predominantly been carried out using tubular or cruciform specimens. Extending the Iosipescu test method for biaxial static and cyclic loading situations would provide a simple, cost effective, and more realistic testing methodology for flat specimens.

Table 2-1: Comparative Study: Evaluation of the (a) torsion of a hoop wound tube (b) biaxial stressing of a tube (c) Off- axis tension (d) Iosipescu test (e) Picture frame (f) Rail shear (g) 45° tests [31].

Criterion	Test						
	a	b	c	d	e	f	g
Can test general laminates	×	×	×	✓	✓	✓	×
Negligible stress concentrations	?	?	✓	×	×	×	✓
Large uniform shear region	✓	✓	✓	×	×	✓	✓
Low cost	×	×	✓	?	?	?	✓

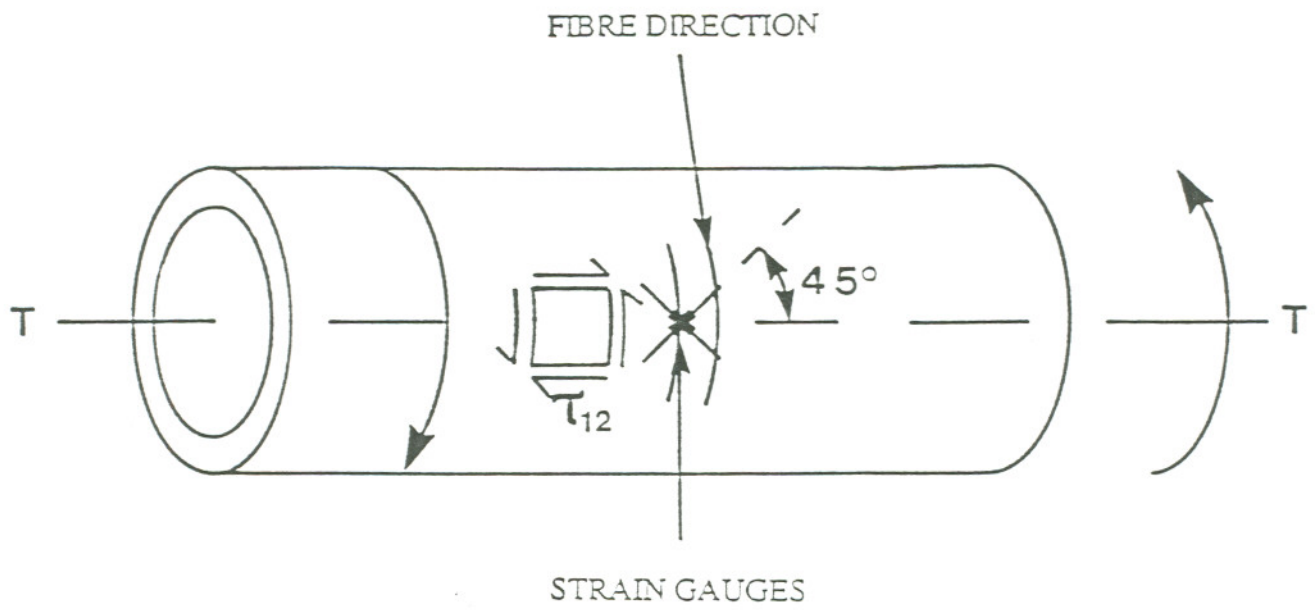


Figure 2-1: Tube torsion test.

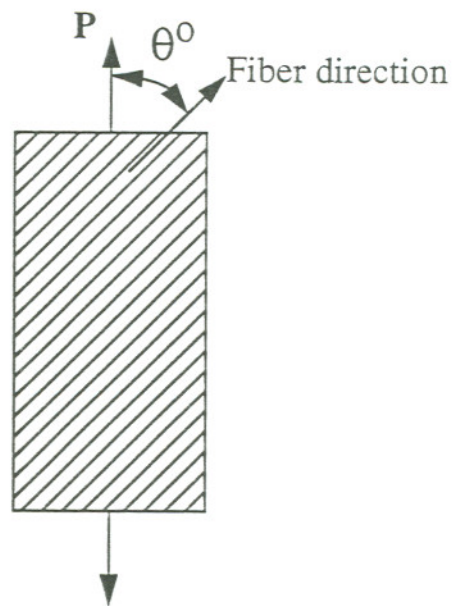


Figure 2-2: Off-axis test.

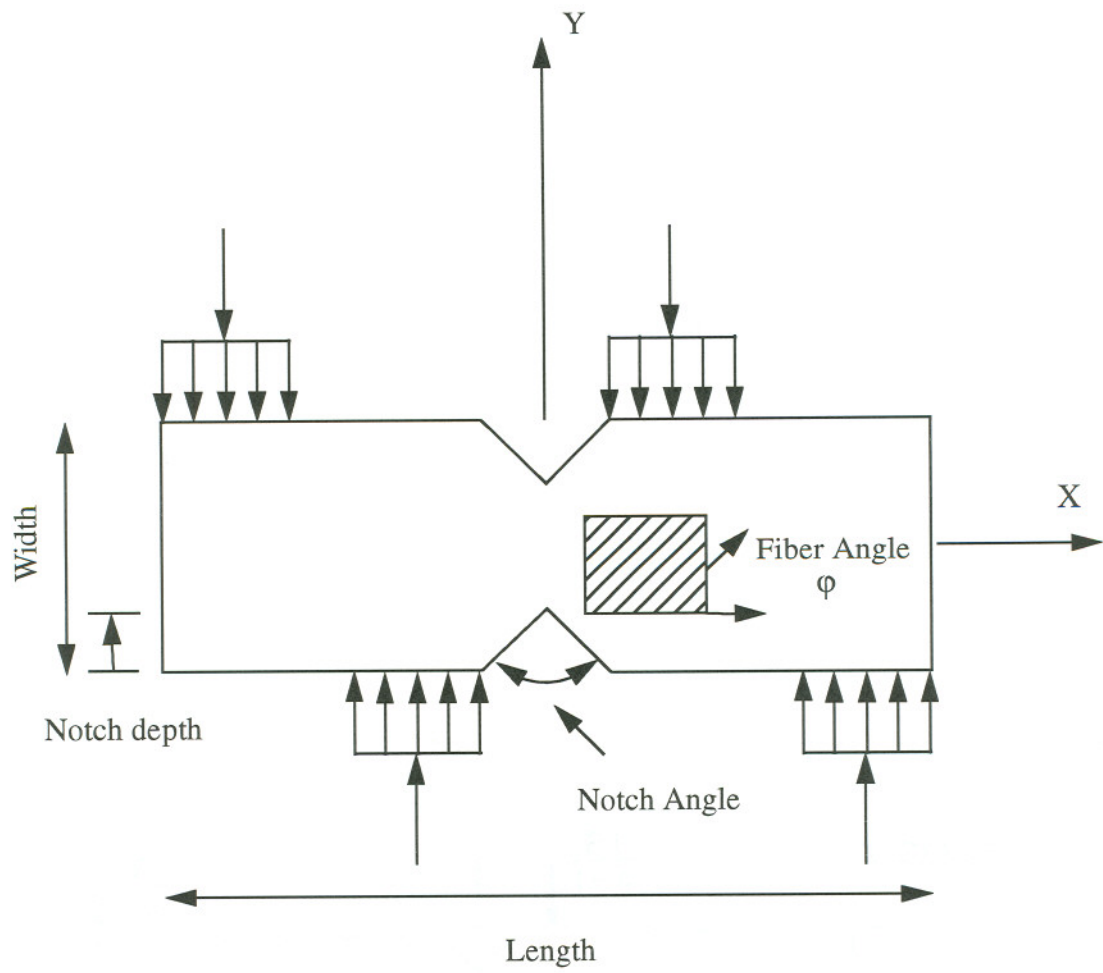
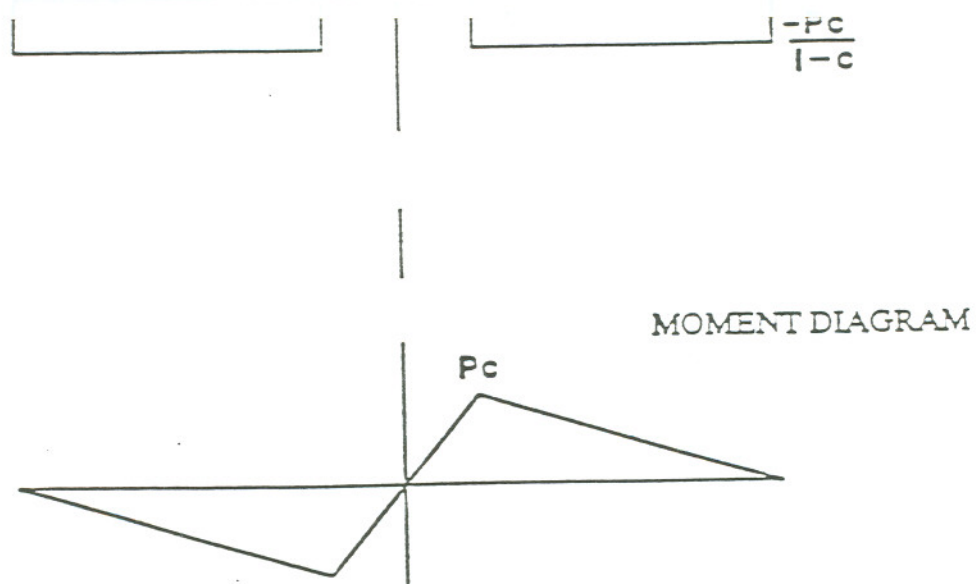


Figure 2-3: Iosipescu shear test.



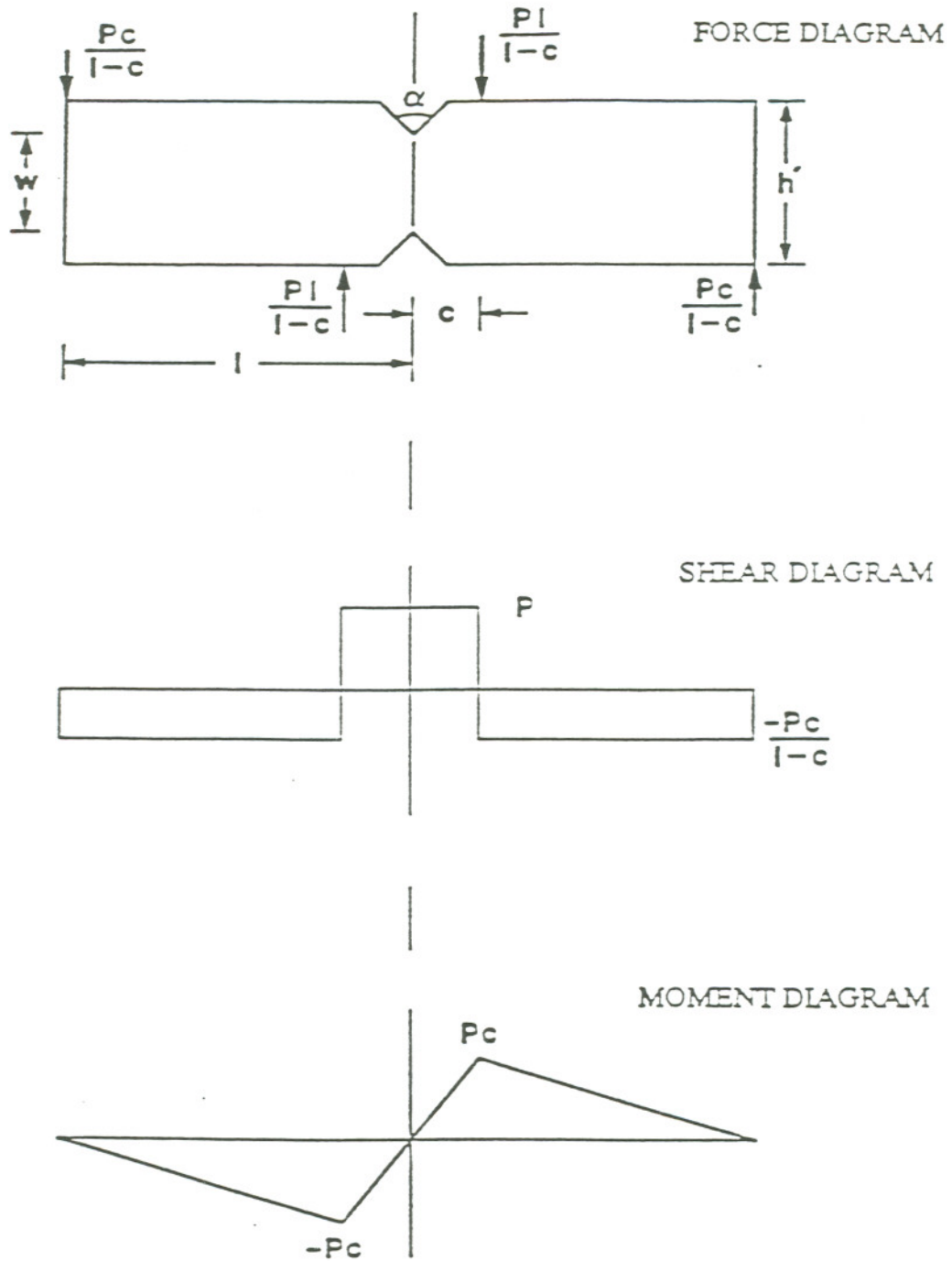


Figure 2-4: Force, Moment, and Shear diagram for the Iosipescu specimen

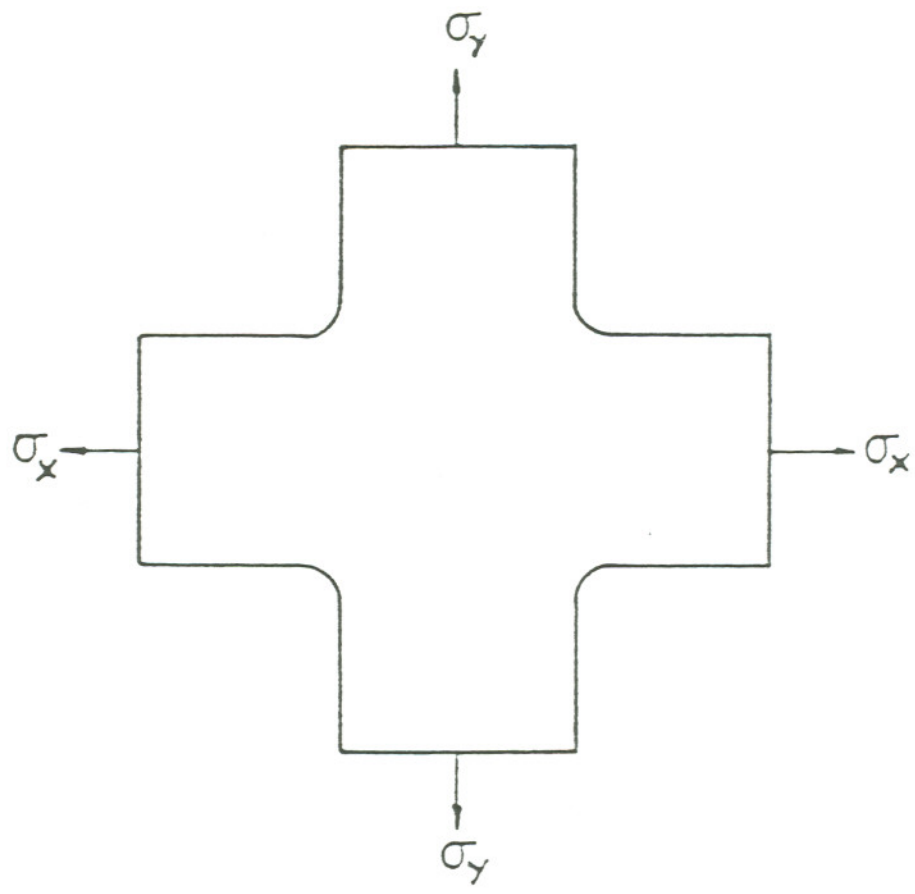


Figure 2-5: Cruciform specimen

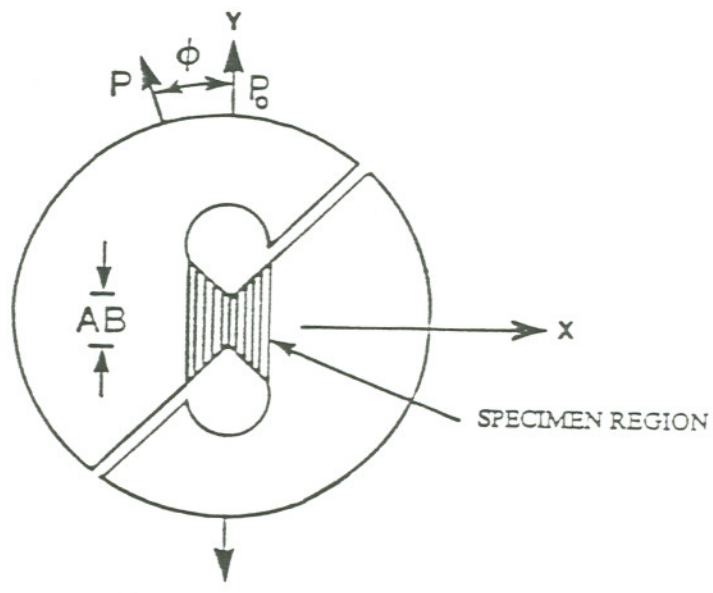


Figure 2-6: Arcan specimen

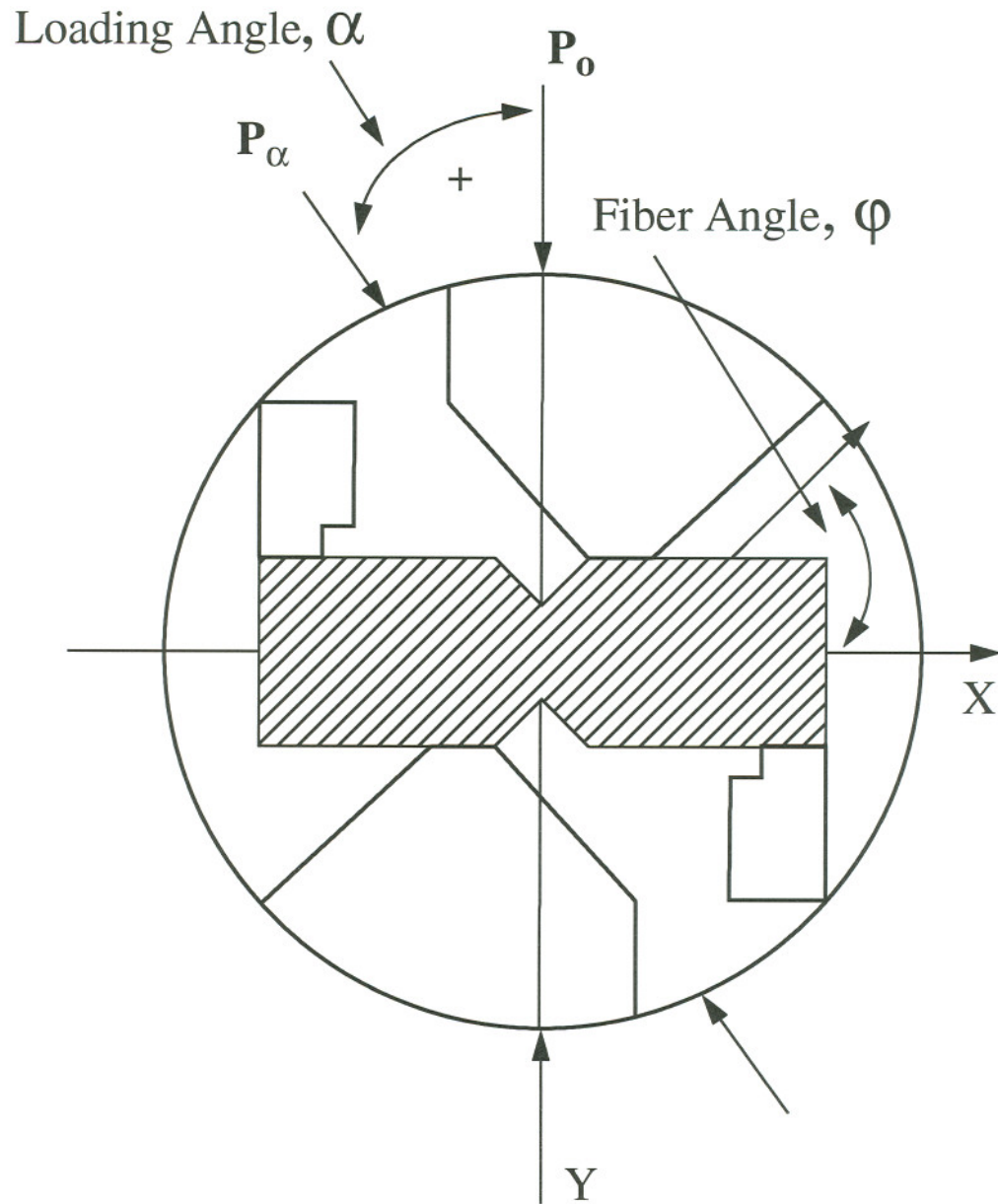


Figure 2-7: Loading configuration in the biaxial Iosipescu test fixture

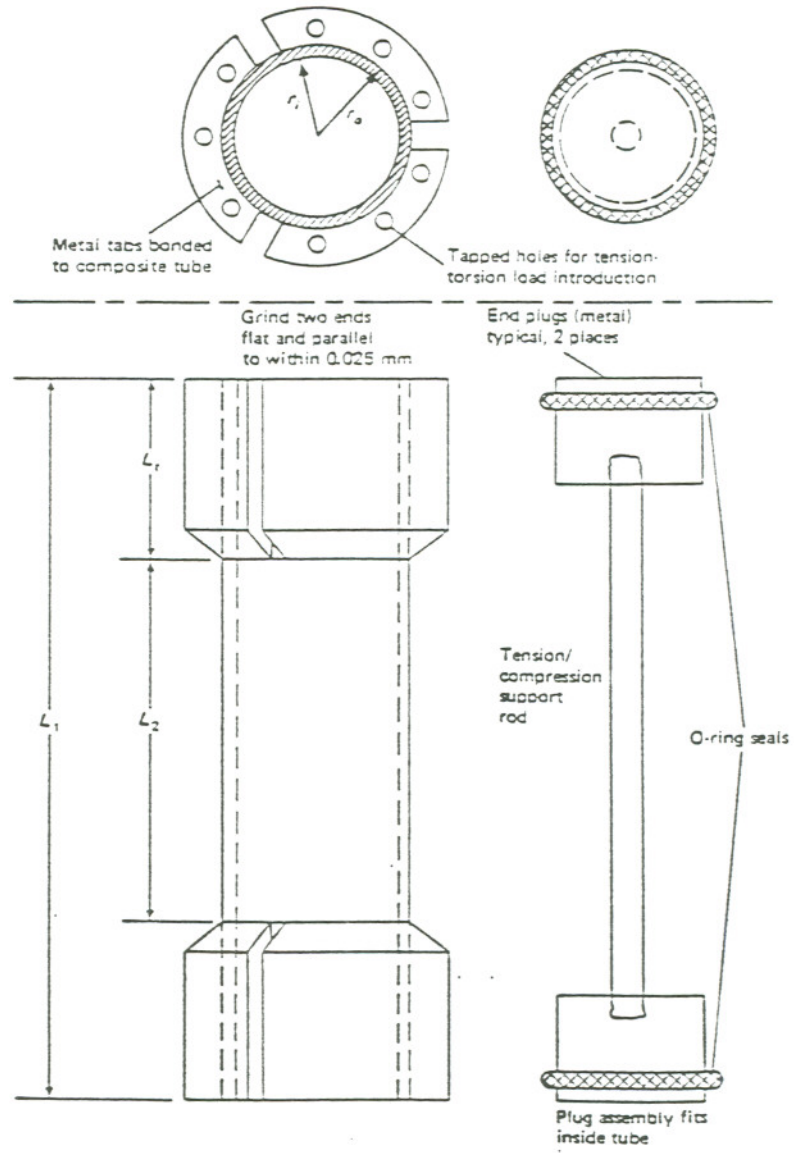
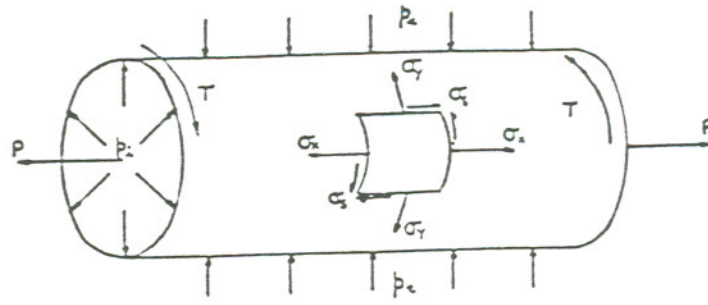


Figure 2-8: Biaxial loading configuration of tubular specimens

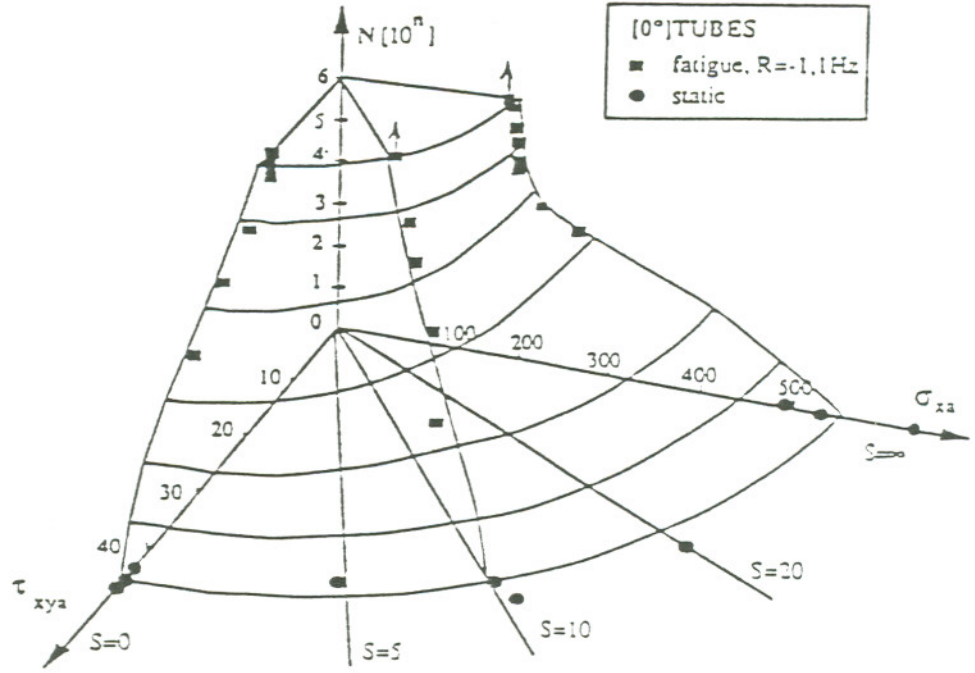


Figure 2-9: Biaxial fatigue failure envelope for Glass/epoxy composite [51].

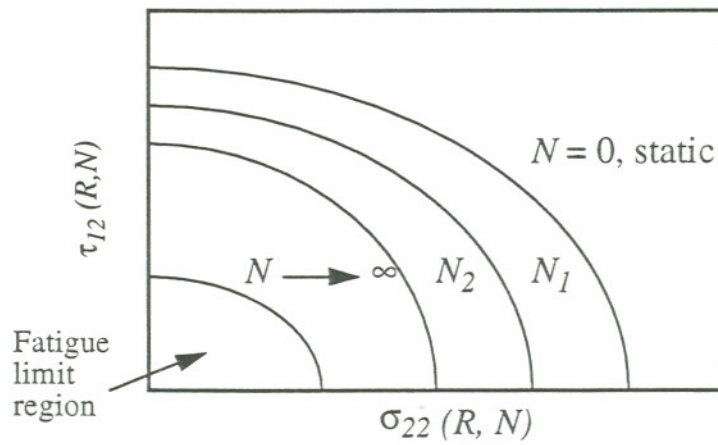


Figure 2-10: Isochronous plots for biaxial fatigue failure representation [52].

Chapter 3

Experimental Details

3.1 Biaxial Iosipescu Test Fixture

The biaxial test fixture is based on the Iosipescu shear test and Arcan test. The fixture is capable of simulating a pure shear stress state, and a wide range of biaxial stress state (shear/transverse-tension or shear/transverse-compression) within the specimen gage section. A detailed description of the fixture can be found in References [2] and [36].

A photograph of the fixture is shown in Figure.3-1. The fixture consists of two halves, each providing two of the loading points necessary for Iosipescu type loading, and the specimens are sandwiched between the two halves, when tested. Each half measures about 100 mm in width, and one half remains stationary and the other half moves parallel and vertical to the stationary half, upon loading. The four loading plates are 10 mm long, and can be adjusted by means of horizontal screws to accommodate specimens as thin as 1 mm. In addition, the position of the loading plates with respect to the notch-root axis of the specimen can be altered to accommodate specimens with various notch geometries. To enable angular loading of the specimen for biaxial testing, both halves consist of two interlocking circular disks. These two disks interlock via a circular groove which enables 360° rotation of the specimen. The angle is set via a 5° graduated scale marked on the exterior circumferential edge of the disks. Securing screws are used on the interlocking disks to maintain the load orientation throughout the duration of the test. In addition, both halves of the fixture have a 30 mm diameter hole at their respective centers, which enables strain gage attachments, and visual observation of the specimen mid-section during testing. Further, the movable half of the fixture is supported by springs and hence speci-

mens can be loaded in fatigue for both shear and biaxial loading cases.

The specimens can be rotated from -45° to $+45^\circ$ (loading angle α) with respect to the external loading axis. Loading at 0° induces pure shear loading, while for other loading angles a biaxial stress state is induced in the specimen. As a convention, the loading angle α is taken to be positive for shear-compression (counter-clockwise rotation) loading and negative for shear-tension (clockwise rotation) loading.

3.2 Test Methodology

In this research, the composite systems were tested for their inplane shear and biaxial properties using the biaxial Iosipescu test fixture. The traditional Iosipescu test employs 0° specimens ($\varphi = 0^\circ$ with fibers oriented along the longitudinal axis of the specimen) or 90° specimens ($\varphi = 90^\circ$ with fibers oriented along the vertical axis of the specimens). A biaxial stress state is induced by rotating the specimen with respect to the external loading axis (Refer Figure.2-7). Based on the force equilibrium, the stresses at the center of the specimen were calculated to be [2]:

$$\sigma_{xx} = \sigma_{yy} = \frac{P_\alpha}{A} \sin \alpha \quad (3-1)$$

$$\tau_{xy} = \frac{P_\alpha}{A} \cos \alpha \quad (3-2)$$

where P_α is the external load, A is the cross-sectional area between the two notches, and α is the loading angle. The angular range of loading in this test is limited to $|\alpha| < 45^\circ$, since stress concentrations become appreciable for larger angles.

So far, the biaxial Iosipescu test has only been used for strength characterization of specimens with fibers aligned along the longitudinal axis (0° specimens) or along the notch root axis (90° specimens) [2,14,18,21,36,53]. However, by changing the fiber ori-

entation with respect to the longitudinal axis of the specimen (angle ϕ in Figure.2-7), a variety of biaxial stress states can be achieved at the specimen mid-section. This approach will necessitate conversion of stresses from the reference coordinate system (X-Y in Figure.2-7) to the material coordinate system. Assuming that equations (1) and (2) hold good, the following equation is obtained:

$$\begin{bmatrix} \sigma_{xx}^{mat} \\ \sigma_{yy}^{mat} \\ \sigma_{xy}^{mat} \end{bmatrix} = \begin{bmatrix} \frac{P_{\alpha} \sin \alpha}{A} + \sin 2\phi \frac{P_{\alpha} \cos \alpha}{A} \\ \frac{P_{\alpha} \sin \alpha}{A} - \sin 2\phi \frac{P_{\alpha} \cos \alpha}{A} \\ \cos 2\phi \frac{P_{\alpha} \cos \alpha}{A} \end{bmatrix} \quad (3-3)$$

where σ_{ij}^{mat} are stresses in the material coordinate system. A plot of realizable normal and shear stresses and the biaxiality stress ratios is shown in Figures. 3-2 to 3-4. It can be observed that the ratio of normal to shear stresses in the material coordinate system can be varied from pure shear to pure transverse-compression or tension. *Thus, by aligning the fibers in a coordinate system other than the reference coordinate system, the ratio of nor-*

mal to shear stresses can be varied in the range $-\infty < \frac{\sigma_{yy}}{|\tau_{xy}|} < \infty$. Broughton [2] has deter-

mined that the apparent shear modulus estimated from such a testing procedure, with off-axis Iosipescu specimens, are in good agreement with analytically determined values for a carbon-epoxy composite system.

3.3 Experiments

3.3.1 Test Materials

Three different composites systems have been studied in this investigation; 1) Silicon carbide fiber reinforced Titanium (SiC/Ti) metal matrix composite, 2) E-glass fiber reinforced polymer matrix composite, and 3) Carbon fiber reinforced epoxy composite. The Ti-SiC composite material was provided by GE Aircraft Engines, Cincinnati. The glass-polymer composites were provided by GlasForms., Inc, San Jose, CA and the Carbon-epoxy composite was provided by CIBA GEIGY LTD, U.K.

3.3.2 Mechanical Tests

Shear and biaxial tests were performed by changing the loading angle for all the three composite systems. In addition, biaxial tests were conducted by varying the fiber orientation in the Iosipescu specimens, henceforth referred to as the off-axis Iosipescu test. Biaxial fatigue testing was carried out on the Ti-SiC metal matrix composite. Further details on the experiments can be found in the respective sections where the results are discussed.

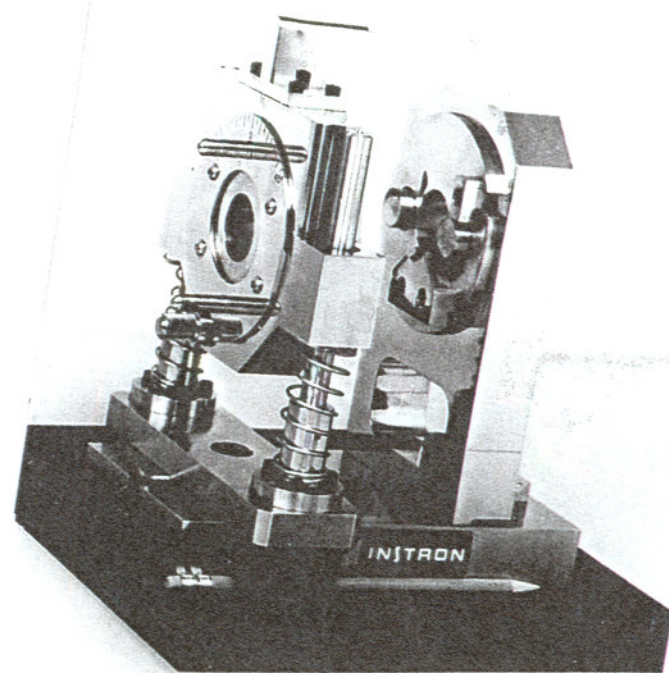


Figure 3-1: Biaxial Iosipescu test fixture.

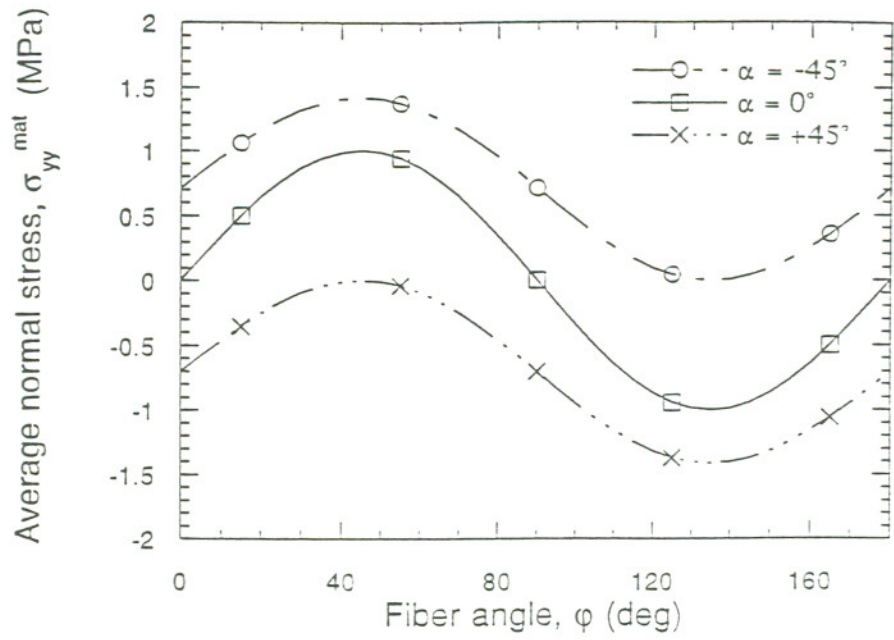


Figure 3-2: Estimated normal stresses using fiber angle variation ($P_\alpha = 12\text{N}$;

$A = 12\text{mm}^2$).

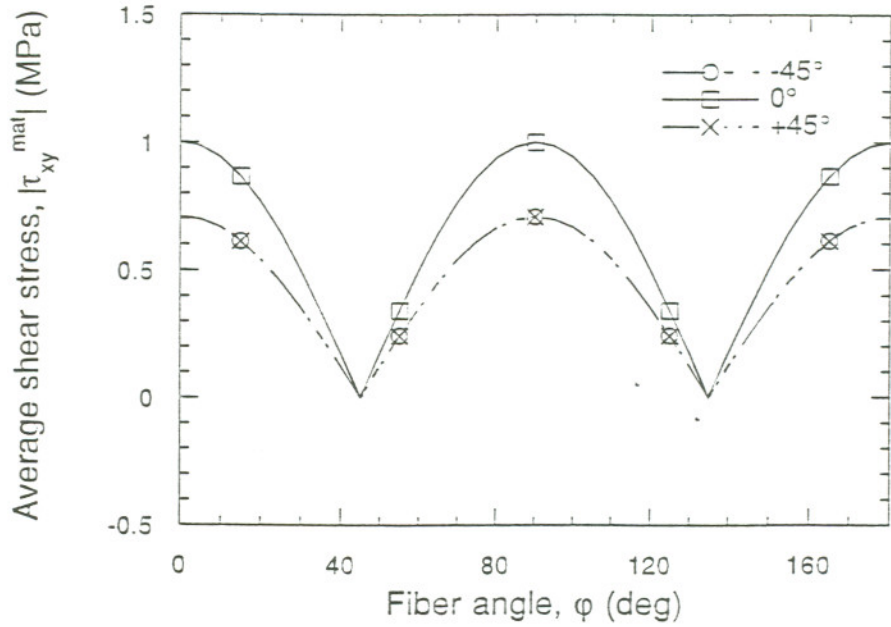


Figure 3-3: Estimated absolute value of the shear stresses using fiber angle variation

($P_\alpha = 12\text{N}$; $A = 12\text{mm}^2$).

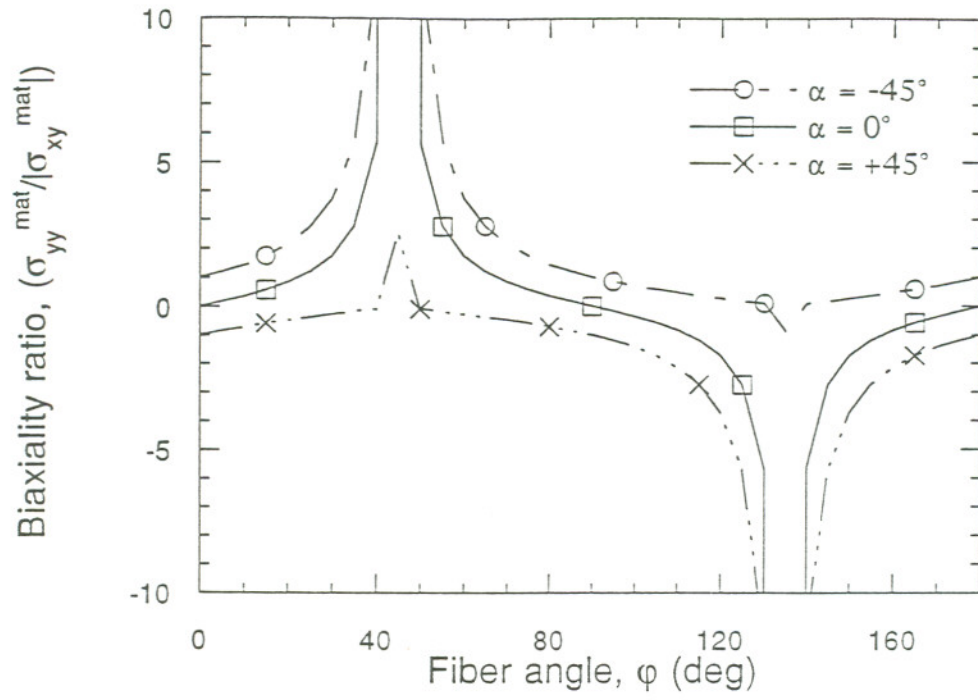


Figure 3-4: Estimated biaxiality ratios using fiber angle variation ($P_\alpha = 12\text{N}$;

$$A = 12\text{mm}^2).$$

Chapter 4

Biaxial Testing of a SiC/Ti Metal Matrix Composite

4.1 Introduction

Metal matrix composites are seriously considered as alternative materials for high temperature applications in aerospace industries. Tailorable mechanical properties combined with high specific properties make them attractive for such uses. Structural applications of these materials demand a comprehensive characterization of their mechanical properties. These include the properties like modulus and strength (along the various directions) and fatigue strength and fracture toughness.

The biaxial Iosipescu test fixture was employed to study the shear, biaxial-static and biaxial-fatigue properties of SiC/Ti-6242 unidirectional metal matrix composite material. The investigation attempted to study the following aspects:

- 1) Shear modulus determination,
- 2) Static failure envelope determination under biaxial loading conditions, and
- 3) Biaxial fatigue characterization.

4.2 Material Tested

The material tested in this study is a SiC fiber reinforced Ti-6242 unidirectional metal matrix composite. The fibers are aligned along the longitudinal specimen axis (0° fiber orientation). The material properties of the fiber and the matrix are shown in Table. 4-1. The fiber volume fraction was approximately 35%. The average notch root radii of

the Iosipescu specimens used in this study, was determined to be 321 μ m.

The biaxial tests were conducted on an Instron (1230-30) universal testing machine with a load capacity of 20000 lbs. The static tests were performed under stroke control mode by applying monotonic compressive loads at a constant ramp rate of 0.0001 in/sec. The fatigue tests were performed under load control mode by applying cyclic sinusoidal compressive loads. Unidirectional composite specimens with 0° fiber orientation fail by the formation of axial splits, originating at the notch roots and extending away from the loading points. A travelling optical microscope was used to monitor and measure the crack (split) length.

A three element stacked rosette strain gage (Micro-measurements WA-06-030WR-120 or WA-03-030WR-120) was used to measure strains. The gage were mounted on one face of the specimen, at the center of the specimen. One gage was used for each specimen. The strains were continuously monitored using a strain amplifier system along with the VIEWDAC data acquisition system. Some specimens were initially polished to 30 μ m diamond, on one side, for mounting the strain gage, while other specimens were tested in the as- received condition.

The static tests were performed under pure shear and shear/transverse tension loadings i.e., at 0°, -15°, -30° loading angles. The fatigue tests were conducted under pure shear and shear/tension loadings at, 0°, -15°, and -35° loading angles.

4.2.1 Static Testing

The static testing in pure shear (0° loading angle) yielded the apparent in-plane shear modulus, G^*_{12} and the shear strength, τ^*_{12} of the tested material. The specimens tested in both pure shear and shear/tension failed by the formation of the axial splits along the fibers near the notch roots. The splits extended away from the two inner loading

points. A plot of the shear stress -shear strain diagram obtained from the pure shear test is shown in Figure. 4-1. The formation of the splits manifested as two successive load drops in the load-displacement diagram. A typical plot of the load-displacement diagram is shown in Figure. 4-2. Some specimens did not show a distinct second drop in the load (corresponding to the formation of the second split). The load-displacement plot for such tests showed a serrated feature, which can be associated with the micro damage accumulating in the specimen gage section (Figure. 4-3). The load corresponding to the formation of the first axial split was treated as the failure load. From the failure loads, the tensile and shear components were estimated and a failure envelope was generated (Figure. 4-4). The transverse tensile strength value was obtained from the manufacturer. This plot compares well with the Tsai-Hill failure criterion for unidirectional composites.

4.3 Finite Element Analysis

As previously mentioned, it has been shown in the literature [17,20,26] that the shear stress distribution along the notch root axis is not uniform and correction factors need to be employed to evaluate the actual modulus and strength values from the experimentally determined apparent values. For 0° specimens, i.e., fibers oriented in the longitudinal direction, the stresses at the center of the specimen are lower than the average stress across the section. This effect is accentuated for materials with increased orthotropy ratio (E_{11}/E_{22}). Therefore the apparent shear modulus will be higher than the true value. Through FEM analysis, appropriate correction factor for the shear stress distribution can be determined.

Finite element analysis was performed to ascertain the actual stress state in the specimen midsection. A commercial FEM package, ANSYS 4.4a was used for the analysis [54]. The analysis were linear elastic and orthotropic. The material properties used in the FEM analysis is presented in Table. 4-2.

Figures. 4-5 and 4-6 shows the shear and normal stress distribution along the notch root axis. As already mentioned, the shear stresses at the center of the specimen are lower than the average stresses. The stress analysis was performed for an applied force of 12 N which gave an average shear stress value of 1 MPa. Also, there is a characteristic shear stress concentration at 0.5 mm below the notch roots.

From the analysis performed for the various loading angles, the average stresses at the center of the specimen are plotted in Figure. 4-7. It can be seen from the figure that the analytical formula (eqn. 3-1,3-2) used to estimate the shear stress values agrees with the FEM calculated values, while the normal stresses obtained from the two approaches are not in agreement. As the FEM calculated shear stress value matched very well with the analytically calculated value (resulting in a correction factor of 0.99) the apparent modulus can itself be treated as the actual value. The correction factor close to 1.00 can be attributed to the low orthotropy ratio, $E_{11}/E_{22} = 1.5$, of the material.

4.4 Biaxial Fatigue Testing

Fatigue is the phenomenon of mechanical property degradation leading to failure of a material or a component under cyclic loading. The aim of biaxial fatigue testing is to experimentally determine a fatigue failure surface determined by testing the material with varying shear and/or axial tension/compression load amplitudes. This study attempted to ascertain whether such a fatigue failure surface determination is possible by using the biaxial Iosipescu test fixture.

Initially, isotropic Aluminum specimens were tested under pure shear, shear/compression, and shear/tension loading conditions, at a frequency of 10Hz. It was found that fatigue cracks do initiate under biaxial loadings, and the number of cycles for failure decreased with increasing tensile component. It is interesting to observe that the specimens failed with the formation of fatigue cracks along the planes of maximum tensile

stress (characteristic of brittle isotropic materials), which otherwise failed along the notch root axis (characteristic of ductile isotropic materials) under static loading conditions. The results of the tests on Al-6061 T-6 alloy are summarized in the following Table. 4-3.

The initial fatigue tests gave us confidence for testing composite specimens under biaxial fatigue loading. There are two parameters that need be characterized in a biaxial fatigue testing: 1) Stress ratio, R , which is the ratio of the minimum to the maximum value of a particular stress component ($\sigma_{min}/\sigma_{max}$), and 2) Stress partition ratio or the biaxiality ratio, S which is the ratio of the normal to shear stress component σ_{yy}/τ_{xy} , (normal stress/shear stress). In the modified biaxial fixture used for this study, the external loading is always compressive in nature and the fixture configuration translates this compressive load to normal and shear loads in the specimen gage section. As such, the only controllable testing variable is the load ratio and it can be shown that this load ratio is the same as the stress ratio. For our study, the load ratio was approximately 0.05. It can also be easily shown that the stress ratio is dependent on the angle of rotation, α and is simply the tangent of the angle. It should however be mentioned that these parameters were derived by using analytical expressions (eqns. 3-1 and 3-2) for stress partitioning in the Iosipescu specimen.

Tests were conducted in pure shear and shear/tension. One specimen was tested for each of the loading conditions. The number of cycles to initiate a crack (split) at any of the two notch roots was determined by periodically monitoring the notch roots with the aid of an optical travelling microscope. In all these experiments the shear component of the load was held constant and the transverse tensile component increased with increasing loading angle. As already mentioned the stress ratio for both the normal and shear components was about 0.05 and the testing was done at a frequency of 30 cycles/min.

4.5 Results and Discussion

The results of the fatigue testing are summarized in Table. 4-4. It can be seen from the table that the number of cycles to initiate a fatigue crack drastically decreased with increasing transverse tensile component in the biaxial loads. The specimens tested at 0° and -15° did not show a catastrophic failure but the splits continued to grow in the longitudinal direction. An optical micrograph of the axial split developed under fatigue is shown in Figure. 4-8. The specimen tested at -35° loading angle failed with features very similar to that of isotropic specimens i.e., cracks initially originated parallel to the fibers and later shifted towards the plane of maximum tensile stress. The geometry of the failure in the three specimens are schematically illustrated in Figure. 4-9.

The fracture surfaces were examined under both optical and scanning electron microscopes. The specimen tested at -35° failed after about 210 cycles. As already mentioned the crack initially started along the fibers and deviated towards the plane of maximum tensile stress. This can be attributed to the increased tensile component of the load. The fracture surface showed some fiber pull-out. Also the interface layer seems to have degraded in the fibers. The above features are shown in Figures. 4-10, 4-11, and 4-12.

A lateral view of the split developed in the fatigued specimen (0°) is shown in Figure. 4-13. The split jumps from one fiber layer to other interconnected by matrix cracks. A transverse view of the fatigue crack shown in Figure. 4-14. The figure shows extensive fiber damage near the notch root and there are matrix cracks interspersed all along the fracture surface.

4.6 Limitations

The modified biaxial fixture can be utilized to generate fatigue failure surfaces under biaxial loading conditions. However it does have certain limitations. One of the two parameters characterizing the biaxial test namely the stress partition ratio can not be independently controlled. As already defined, the stress partition ratio is the ratio of the normal component of the load to the shear component of the applied load. In a pure shear test the normal component is zero and for tests conducted in shear/tension situations, i.e., negative loading angles, the stress ratio is given by the tangent of the loading angle. Hence, the stress ratio can not be independently varied. The maximum rotation that can be applied is 45° and this gives a maximum stress ratio of 1.00. In other words, a biaxial test can never be conducted in the fixture, for conditions where the tensile component of the load exceeds the shear component. On a fatigue failure surface, this condition will be an area under a line with a slope 1 and the shear stress axis. Hence the fatigue failure surface generated is restricted to loading conditions enclosed within this area.

Another important limitation is that for tests at increasing loading angles, there was excessive specimen slippage. This problem was partly circumvented by placing plexiglas (polymethylmethacrylate-PMMA) pieces on the fixture, which restricted the specimen sliding. However it still needs to be analyzed whether such an arrangement would affect the stress state in the material.

4.7 Conclusions

This work has shown that the modified biaxial test fixture could be used effectively for shear property measurements and biaxial failure envelope generation for unidirectional composite materials. With regard to cyclic testing, though the fixture has limited capabilities, it can still be used for generating a fatigue failure surface.

Table 4-1: Material properties of the Matrix and Fiber

Properties	Matrix	Fiber
UTS, MPa (ksi)	1089 (158.00)	3447 (500.00)
E, GPa (msi)	124 (18.00)	408 (59.2)
0.2% YS, MPa (ksi)	1062 (154.00)	-
Compressive UTS, MPa (ksi)	-	6895 (1000.00)
Density, g/cm ³ (lb/in ³)	4.4 (0.16)	3.0 (0.11)

Table 4-2: Mechanical properties used for the FEM Analysis

Property	Value
E ₁₁ longitudinal, GPa (msi)	223.5 (32.42)
E ₂₂ transverse, GPa (msi)	164.1 (23.80)
G ₁₂ in-plane shear, GPa (msi)	55.6 (8.07)
ν_{12}	0.25
Notch root radius, micron	321

Table 4-3: Biaxial Fatigue Test Results for Al-6061 T-6 alloy.

Orientation	Applied Load Range, $(P_{\alpha}^{max} - P_{\alpha}^{min})$ lbs	No cycles to failure, N
-30° (Shear and Tension)	600	759600
0° (Pure Shear)	600	2007200
30° (Shear and Compression)	600	No failure (stopped after 2.5×10^6 cycles)

Table 4-4: Fatigue Test results for the SiC/Ti metal matrix composite.

Loading Angle, α , in deg	Applied Cyclic Loads, $-P_{\alpha}$ lbs	Shear Load, lbs (from Anal.Exp) $-P_{\alpha} \cos \alpha$	Normal load, lbs (from Anal. exp) $-P_{\alpha} \sin \alpha$	Number of cycles to initiate a crack (at any of the two notch roots), N
0°	600	600.00	0.00	33000
	30	30.00	0.00	
-15°	621	599.84	160.73	14370
	31	29.94	8.02	
-35°	732	599.62	419.86	170
	36	29.49	20.65	

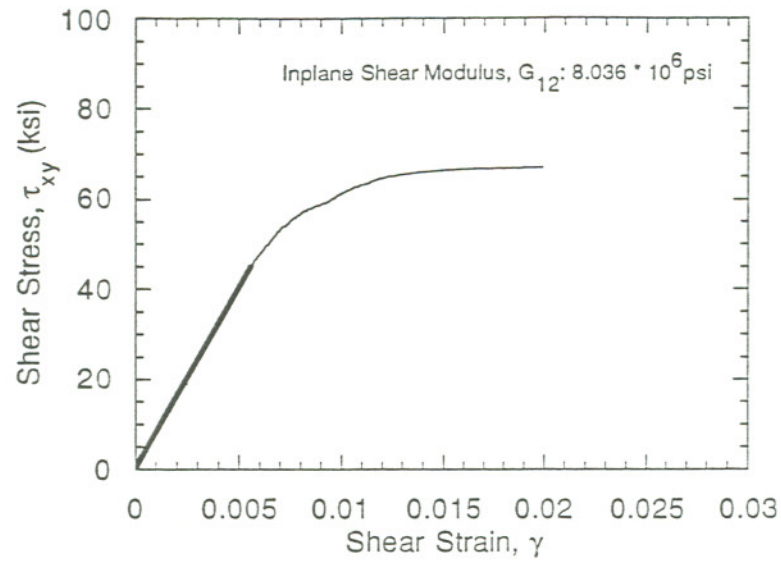
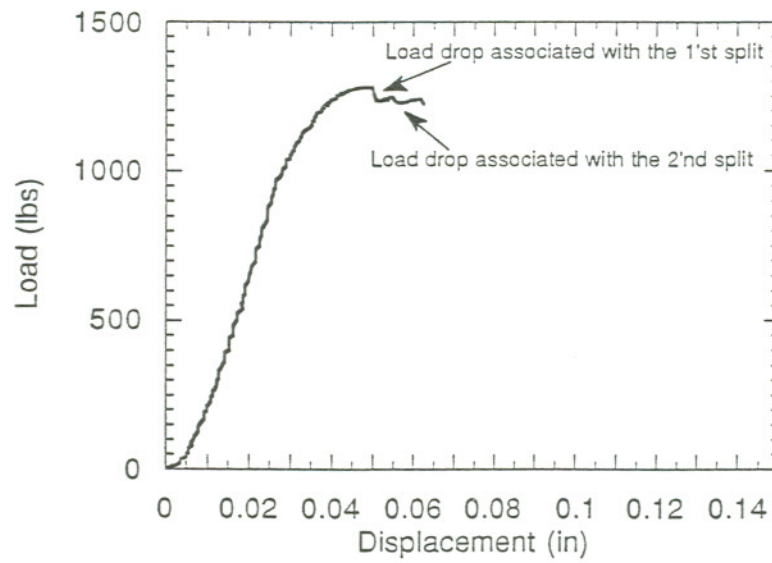


Figure 4-1: Shear stress - strain diagram

Figure 4-2: Load-displacement diagram under static loading: loading angle, $\alpha = 0^\circ$

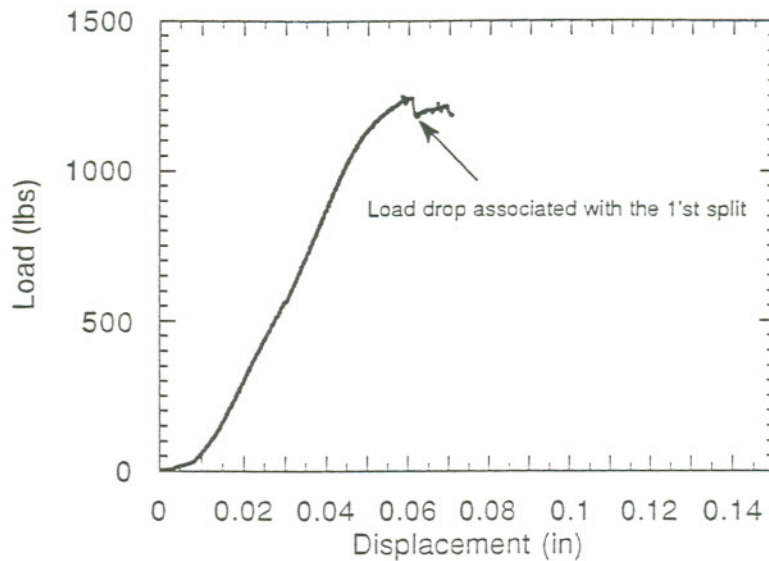


Figure 4-3: Load-displacement diagram under static loading: loading angle, $\alpha = -15^\circ$

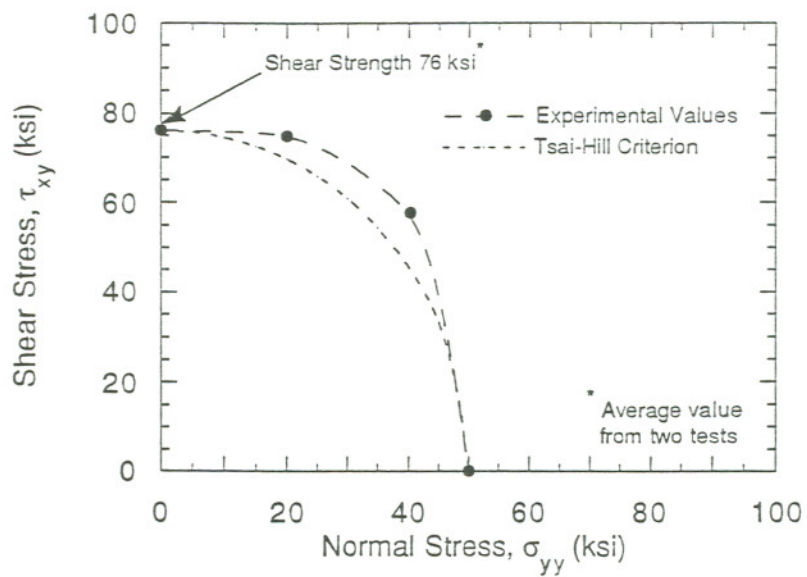


Figure 4-4: Biaxial failure envelope for the tested SiC/Ti metal matrix composite.

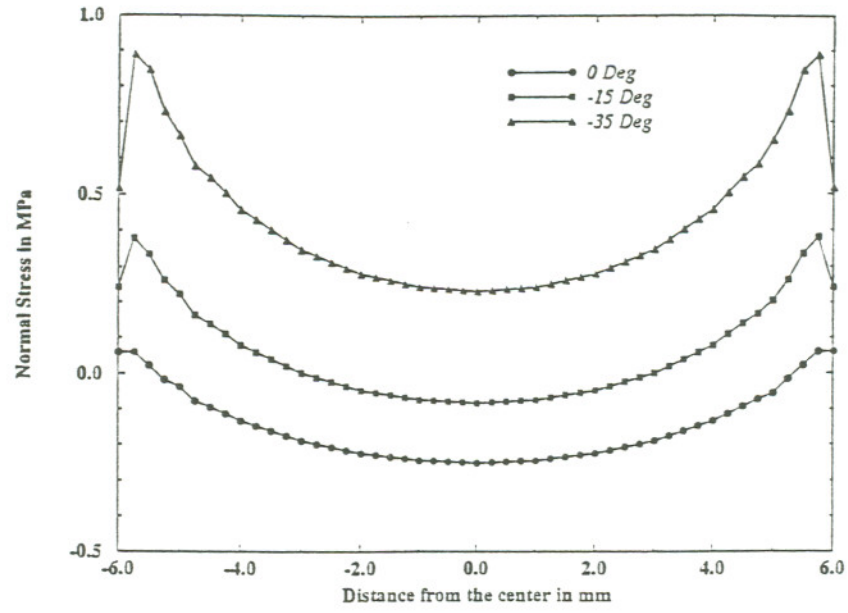


Figure 4-5: Normal stress σ_{yy} , distribution along the notch root axis.

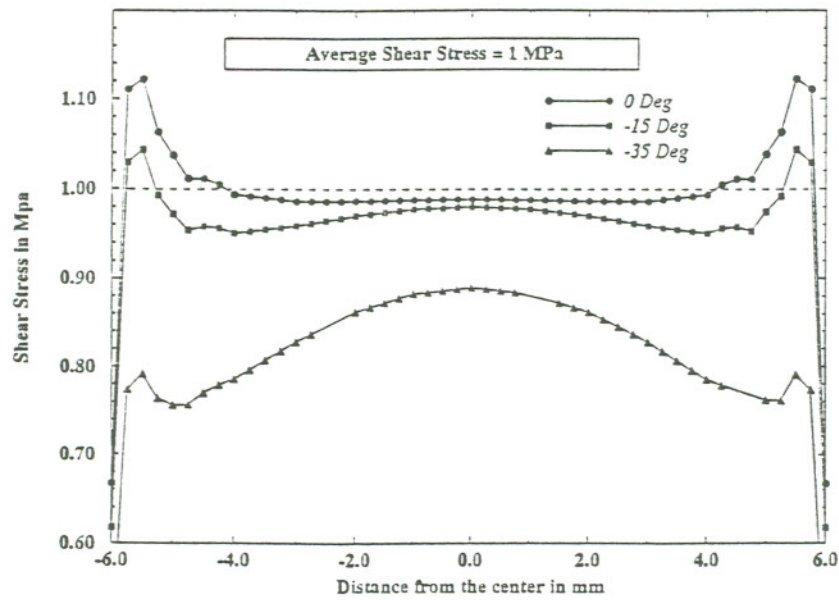


Figure 4-6: Shear stress distribution τ_{xy} , along the notch root axis

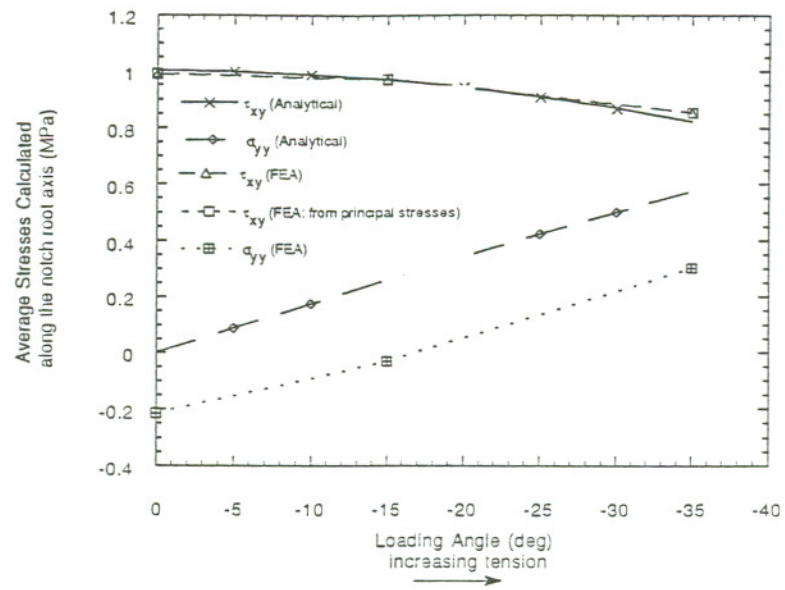


Figure 4-7: Analytical and numerical estimation of average stresses in the specimen

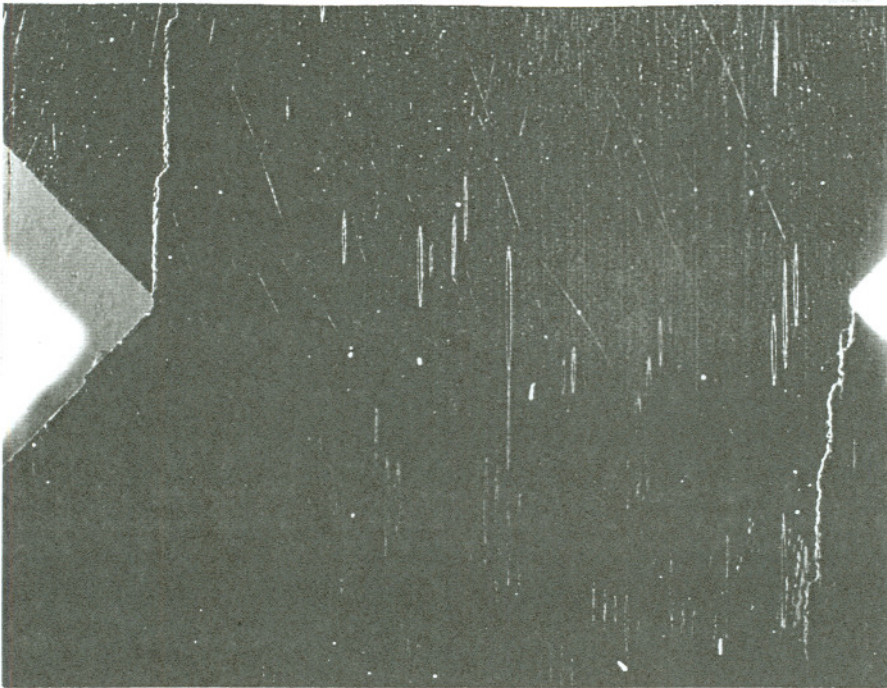
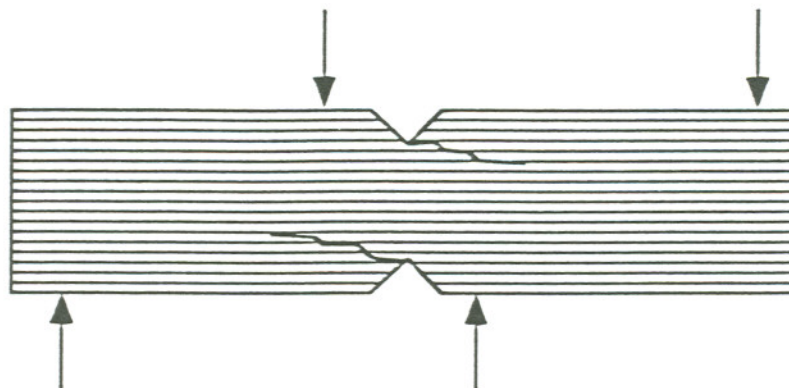
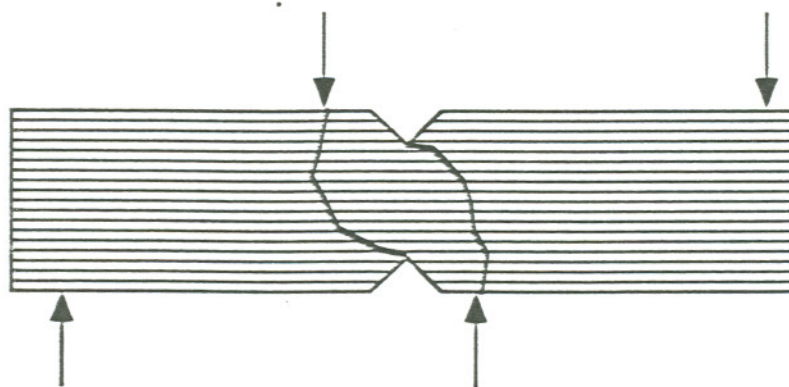


Figure 4-8: Optical micrograph of a specimen loaded in fatigue



(a)



(b)

Figure 4-9: Schematic of the failure modes under fatigue: (a) 0° and -15° loading angle, (b) -35° loading angle

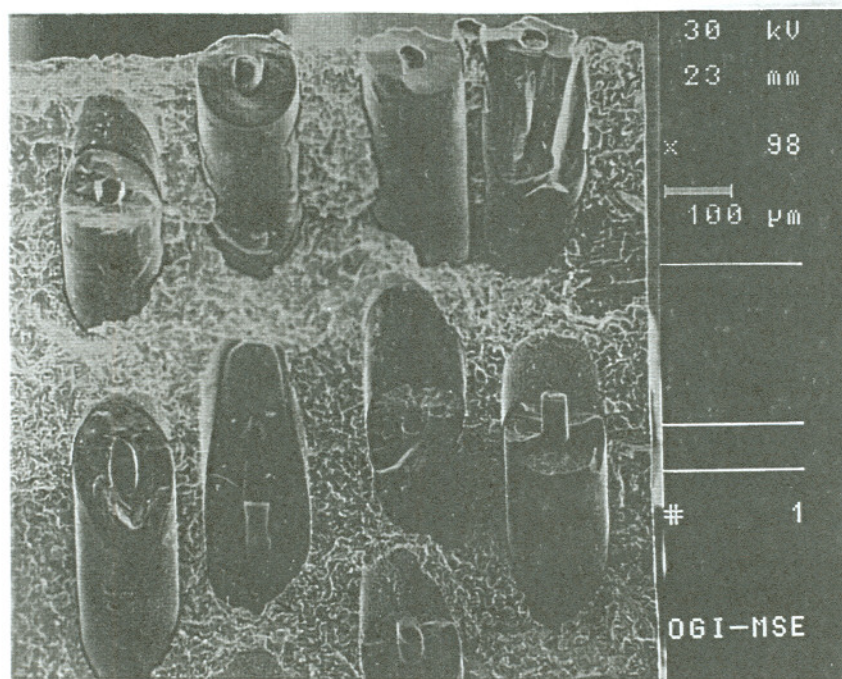


Figure 4-10: SEM micrograph of the fracture surface

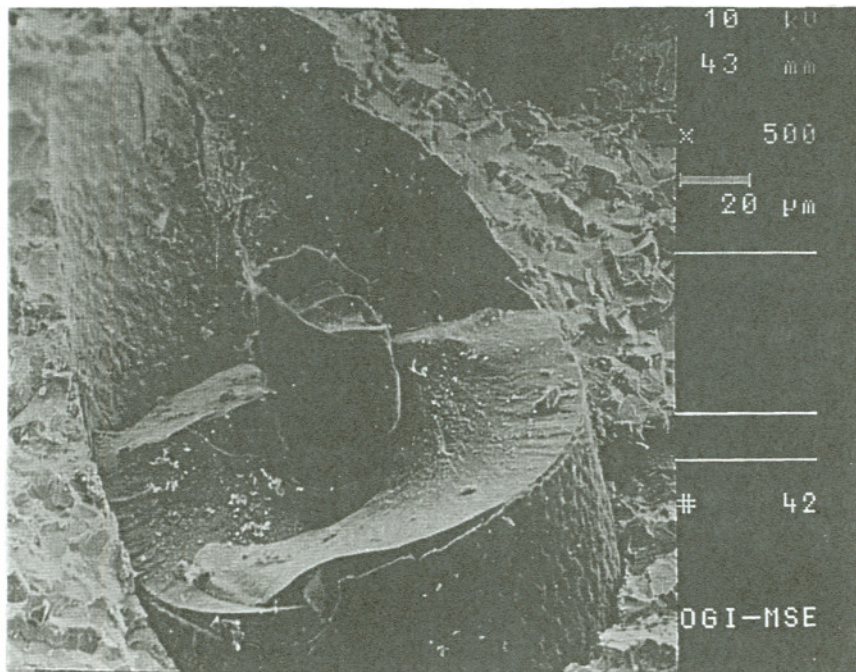


Figure 4-11: SEM micrograph of the fracture surface

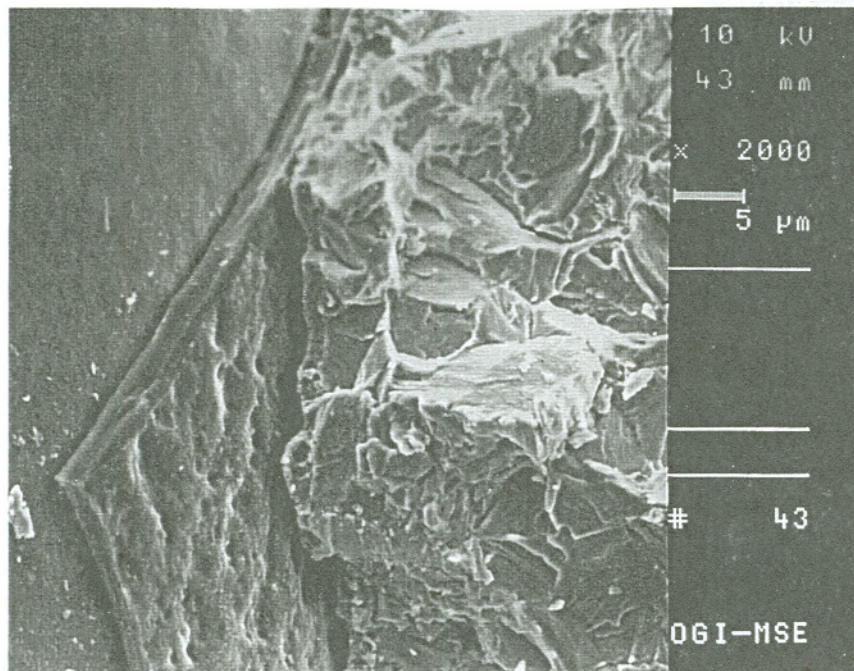


Figure 4-12: SEM micrograph of the fracture surface

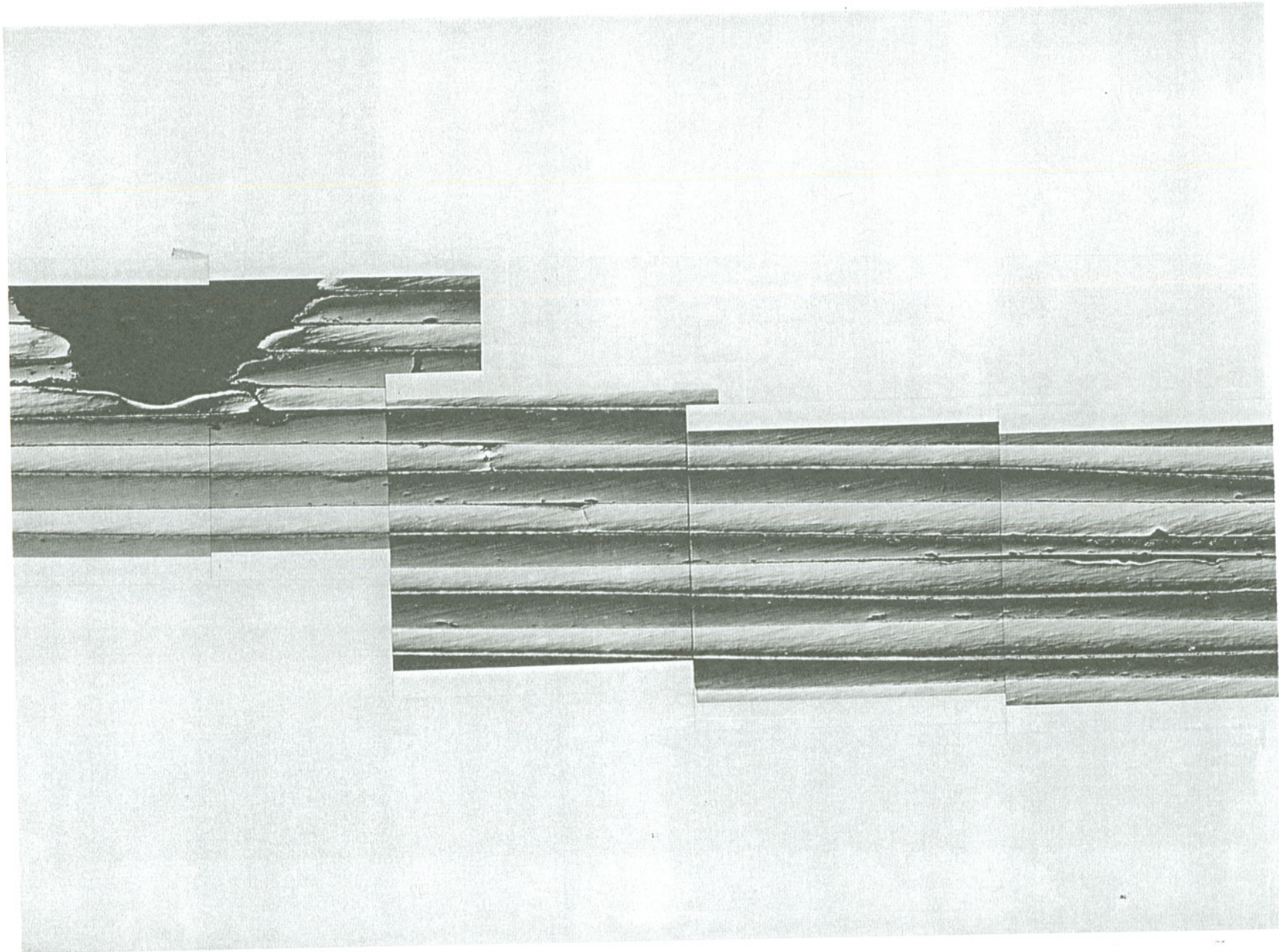


Figure 4-13: Lateral view of the split developed under fatigue

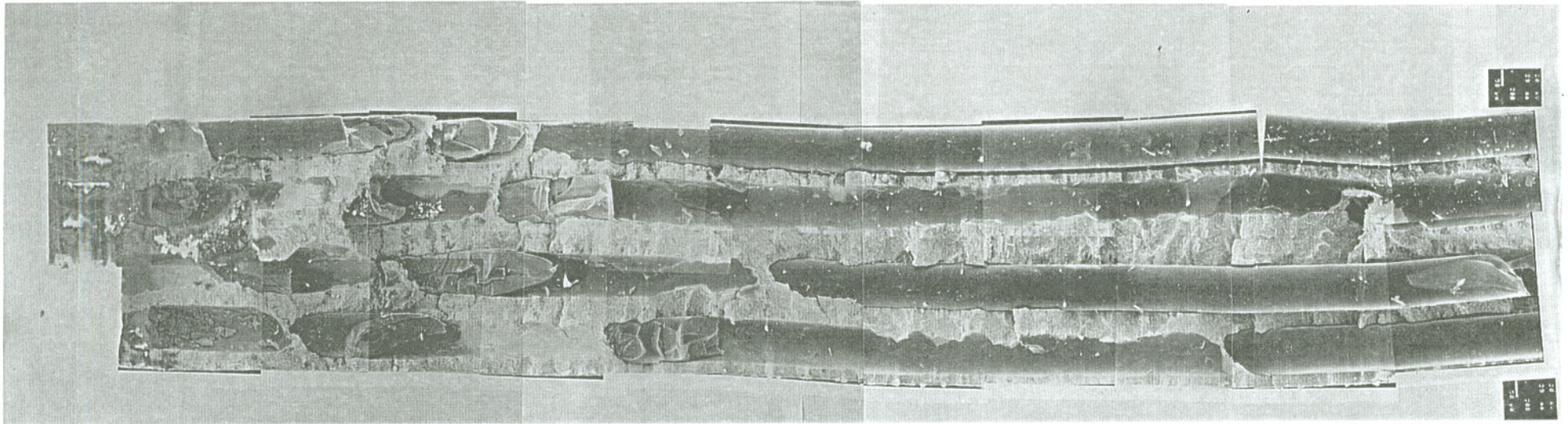


Figure 4-14: Transverse view of the fatigue fracture surface

Chapter 5

Biaxial Testing of Glass Reinforced Polymer(GRP) Matrix Composites

5.1 Introduction

Glass reinforced polymeric matrix composites (GRP) have extensively been used in the area of non ceramic insulators in high voltage transmission lines. These insulators, apart from mechanical and electrical loads, are exposed to moisture from rain and humidity. In general, polymeric materials absorb moisture and their mechanical properties tend to deteriorate with long exposure to moisture [55,56]. It is therefore important to determine the effect of moisture on the strength properties of these materials.

This study is aimed at determining the effect of moisture on the mechanical properties of the commonly used GRP materials. In particular, the study will focus on the effect of moisture on shear and biaxial intralaminar strength properties of GRP materials.

5.2 Material Tested

Three different GRP systems were studied for moisture effects: E-glass/epoxy, E-glass/polyester and E-glass/vinyl ester. These are the commonly used materials for insulator applications. The experimental study involves characterizing the moisture absorption process and biaxial tests on the as-received specimen to establish baseline data for future comparison. In addition, biaxial tests were conducted on fully and partially saturated specimens to determine the effect of the absorbed moisture on the strength properties.

5.2.1 Experimental Procedure

The ambient medium was selected as distilled water. A test temperature of 50° C was chosen. This was done to accelerate the diffusion process. All specimens were machined from unidirectional pultruded composite material supplied by GlasForms, Inc. The fiber orientations were parallel to the plane of the specimens. The unnotched Iosipescu specimens were exposed to moisture as rectangular blanks, to minimize the effect of micro-cracking that may occur while machining.

The specimens were suspended in a glass beaker containing distilled water, with both the sides exposed to water. The entire setup was placed in an incubator maintained at 50° C. The incubator maintained the temperature within $\pm 2^{\circ}\text{C}$. Prior to moisture exposure, the specimens were dried in an oven at 60° C, until no change in weight was observed.

The wet specimens were weighed periodically using a Sartorius analytical balance with an accuracy of 0.0001 g. During the course of the experiment, it was found that it took a longer period of time for the balance to equilibrate when the specimens were directly transferred to the sealable bags and weighed. Therefore, the specimens were transferred to a beaker containing distilled water at room temperature and then transferred to sealable bags after weighing. This ensured that the specimens would reach room temperature quickly and would satisfy the weighing process within the prescribed period of 30 minutes.

5.3 Results

Iosipescu specimens were made from the three systems, and were subsequently tested under pure shear and shear/tension loadings. Biaxial tests (shear and tension) were carried out in the modified Iosipescu test fixture. The specimens were tested under as-

received(dry) and moisture-exposed(wet) conditions. The specimens tested in the as-received condition were to establish baseline data. For the wet specimens, notches were machined and were subsequently tested within a period of six hours in order to minimize any effect of drying.

All the tested specimens failed by the formation of axial splits, and the average load for the formation of axial splits was treated as failure. The failure load for the specimens tested under both wet and dry conditions are shown in Figures. 5-1, 5-2, and 5-3. It can be seen from Figure. 5-2 that for the fully saturated glass-epoxy composite, there is a significant drop in the failure load (about 10-15%) compared to the dry specimens from the same system. For the partially saturated glass/polyester and glass/vinylester system, no significant drop in the failure loads was observed. This may be attributed to the fact that the specimens were not fully saturated.

Even though the tested dry and wet specimens failed by the formation of axial splits, there was a marked difference in the nature of the failure process, especially for the fully saturated glass-epoxy specimens. The formation of axial splits in the dry specimens was instantaneous. The splits initiated at the notch roots, extended along the fiber direction and were subsequently arrested away from the loading points. In fully saturated glass-epoxy specimens, the formation and extension of axial splits occurred at a much slower rate. Further, there was no significant load drop in the load-displacement diagram. A typical plot of the load-displacement diagram for the wet and dry specimens is shown Figure. 5-4. As such, it was difficult to establish the actual load corresponding to the formation of the splits. The specimens were observed for the formation of axial splits by illuminating the gage section with a halogen lamp. Since the glass-epoxy specimens were translucent, the split formation could be observed and the corresponding load value for the initiation of axial splits were marked on the load-displacement diagram.

For both the partially saturated glass-polyester and glass/vinylester specimens, the formation of axial splits was instantaneous. In the partially saturated glass/vinylester spec-

imens however, some discoloration of the matrix could initially be observed at the notch roots prior to the formation of axial splits. This can be explained on the basis of the effect of moisture distribution inside the material. The tested glass-polyester and vinyl ester specimens were exposed to moisture for a period of 2 months as opposed to 6 months for the fully saturated glass-epoxy specimens. A plot of moisture distribution inside the material (as a function of exposed time), is shown in Figures. 5-5, 5-6, and 5-7. The independently estimated D and M_m values were used to generate these plots. In the partially saturated specimens the moisture distribution through the thickness is not uniform. Further, there is a significant portion at the center of the specimen which has a much lower moisture concentration than the regions close to the external surfaces. Hence, the surface layer might fail by the influence of increased moisture preceding the interior.

The normal and shear stresses at failure were calculated using the equations 3-1 and 3-2. The results are plotted as a failure envelope for the three systems (Figures. 5-8, 5-9, and 5-10). A comparison of the failure envelopes for the three systems tested under dry condition is given Figure. 5-11. It can be seen from this diagram that the glass/vinylester system seems to have the highest resistance to axial splitting whereas the glass/polyester composites show a much lower resistance to this type of failure.

5.4 Conclusions

From the mechanical tests performed, the following conclusions can be drawn. E-glass/polyester system showed the lowest resistance to axial splitting, while the glass vinyl ester system showed highest resistance to axial splitting. The fully saturated glass/epoxy system failed at significantly lower loads compared to that of the dry specimens. Further, the nature of axial split formation markedly differed in the fully saturated glass-epoxy composite in comparison to the dry material, indicating that the epoxy matrix was substantially affected by the absorbed moisture. The reduction in the failure loads was approximately 10 - 15%. In the partially saturated glass/polyester and glass/vinylester systems, no significant effect of absorbed moisture on the failure properties was observed.

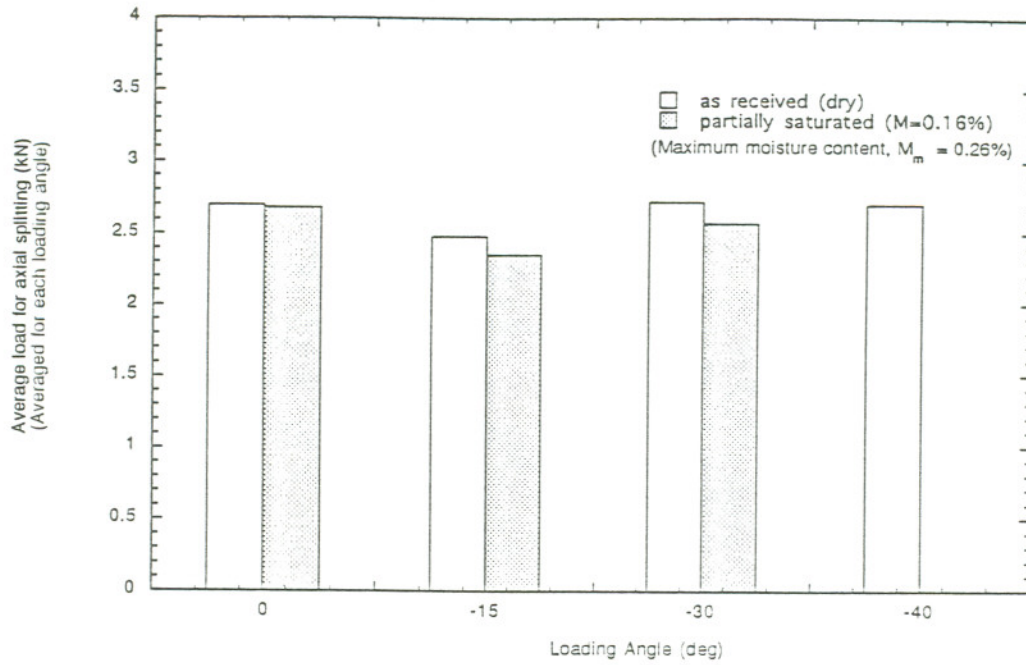


Figure 5-1: Biaxial Failure loads for E-glass/vinylester system

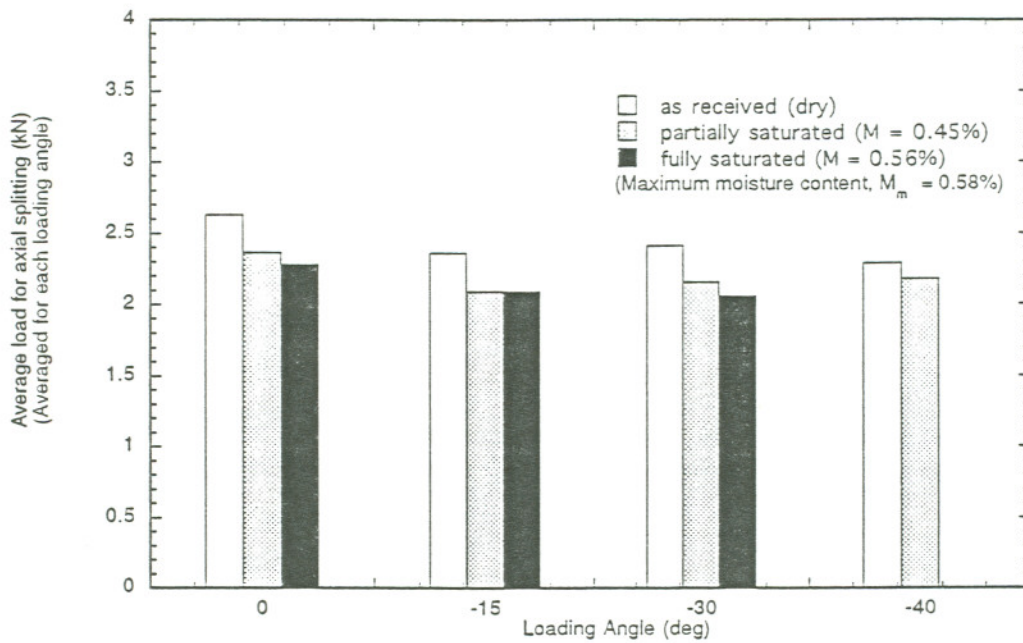


Figure 5-2: Biaxial Failure loads for E-glass/epoxy system

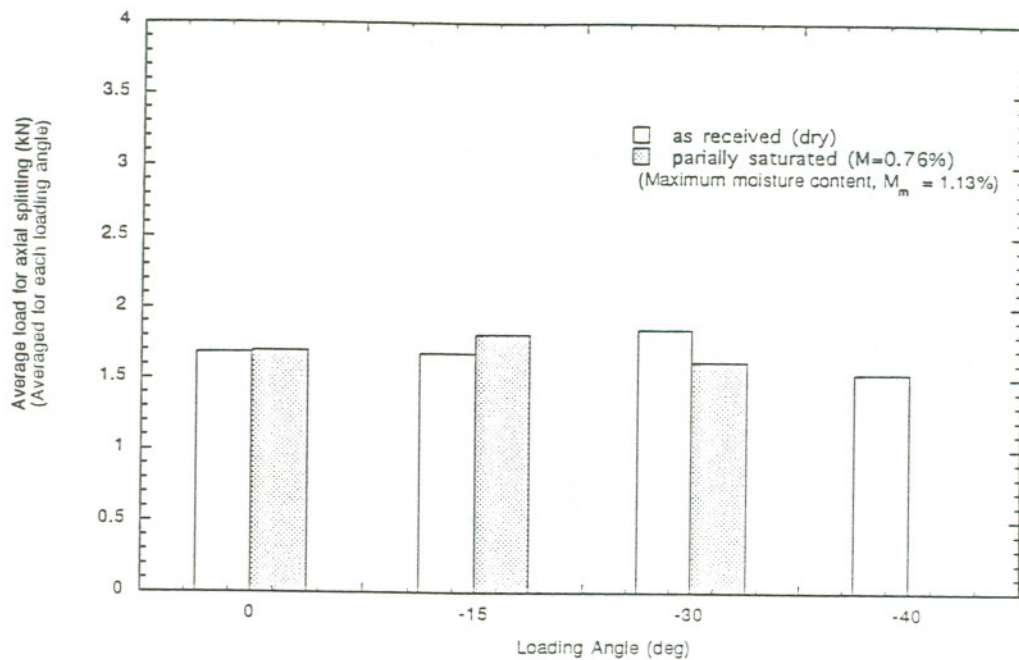


Figure 5-3: Biaxial Failure loads for E-glass/polyester system

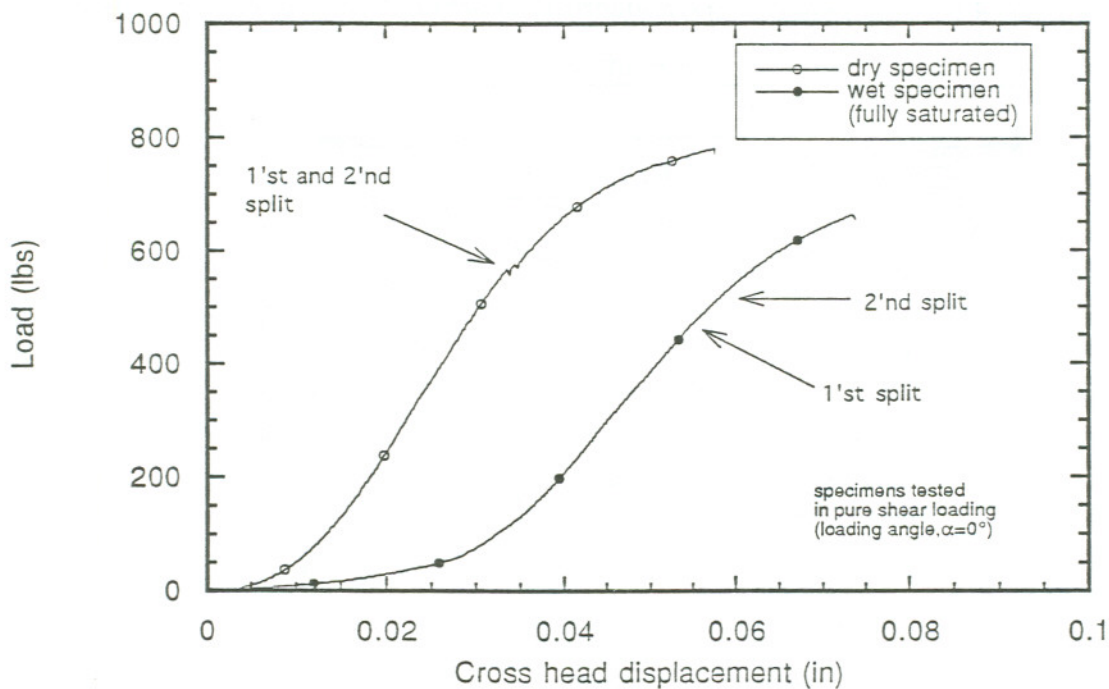


Figure 5-4: Load-displacement plots for dry and wet E-glass/epoxy specimens

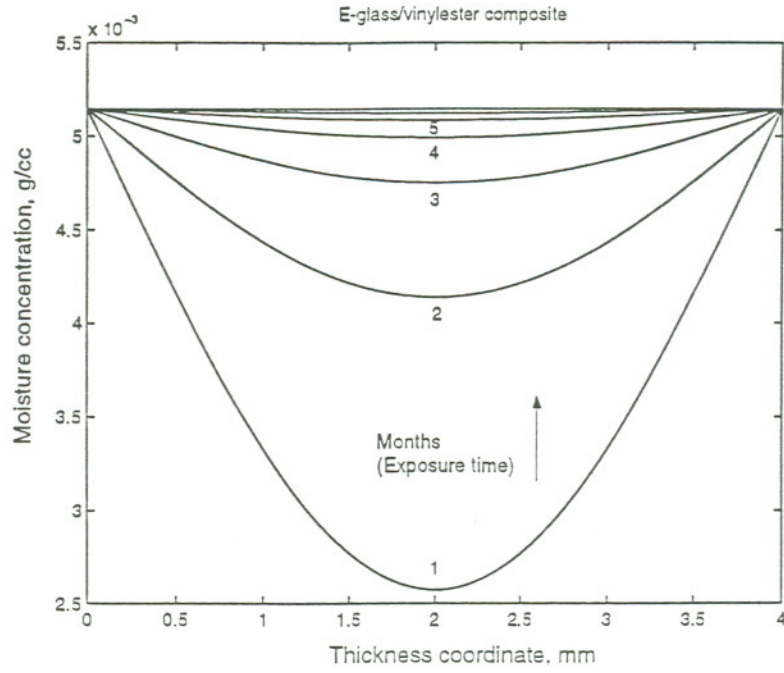


Figure 5-5: Variation of moisture distribution with exposed time for E-glass/vinylester composite.

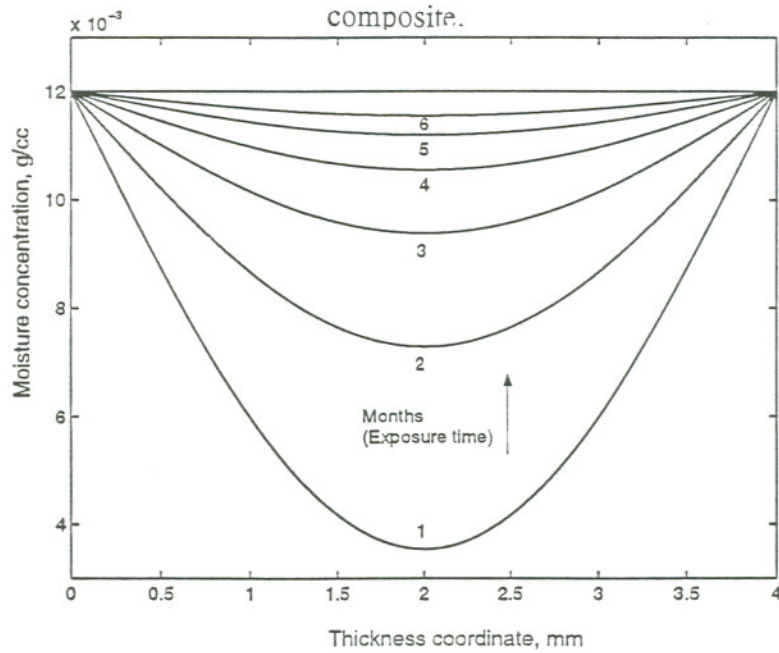


Figure 5-6: Variation of moisture distribution with exposed time for E-glass/epoxy composite.

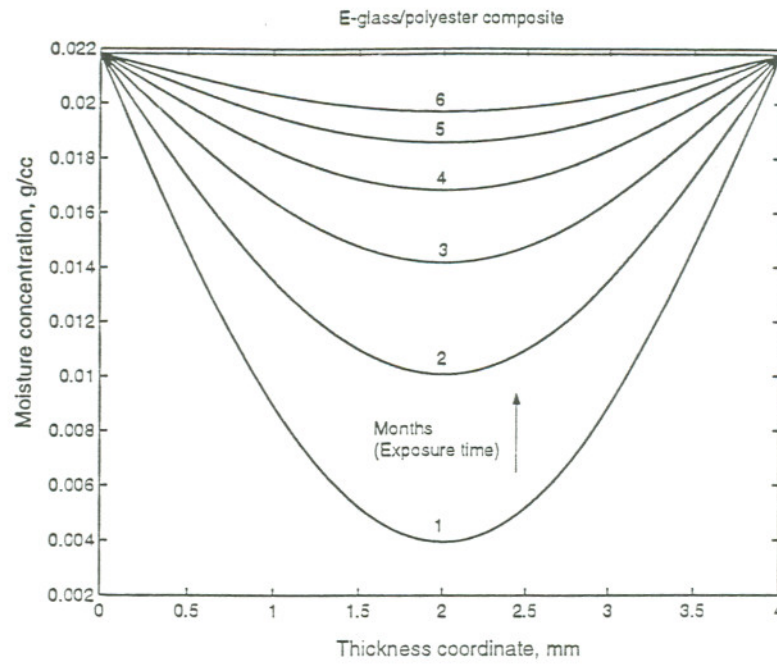


Figure 5-7: Variation of moisture distribution with exposed time for E-glass/polyester

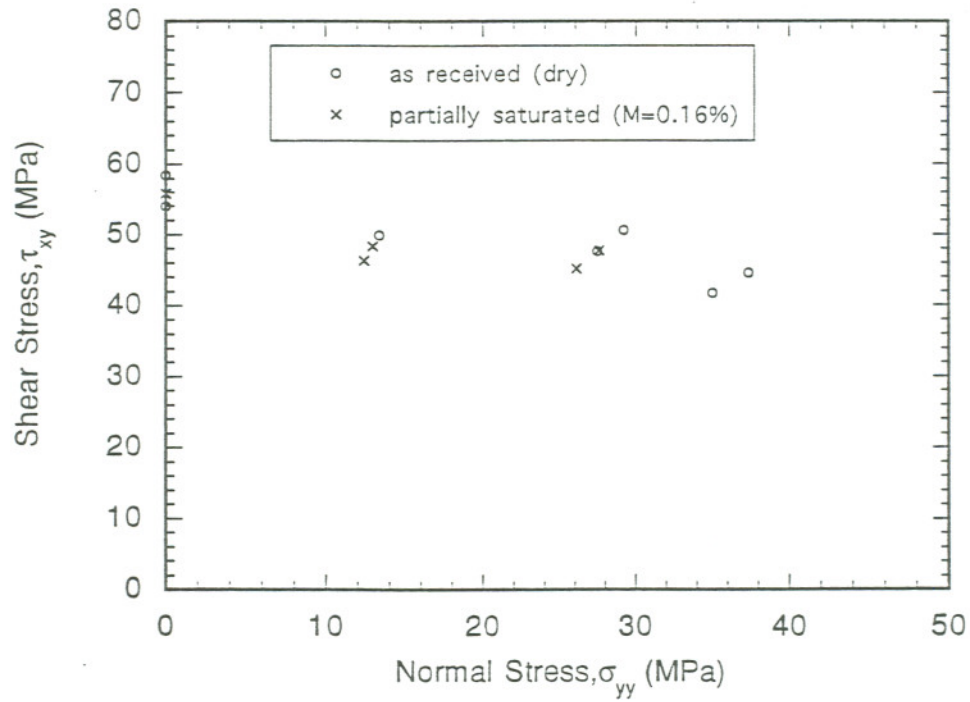


Figure 5-8: Biaxial failure envelope for E-glass/vinylester system

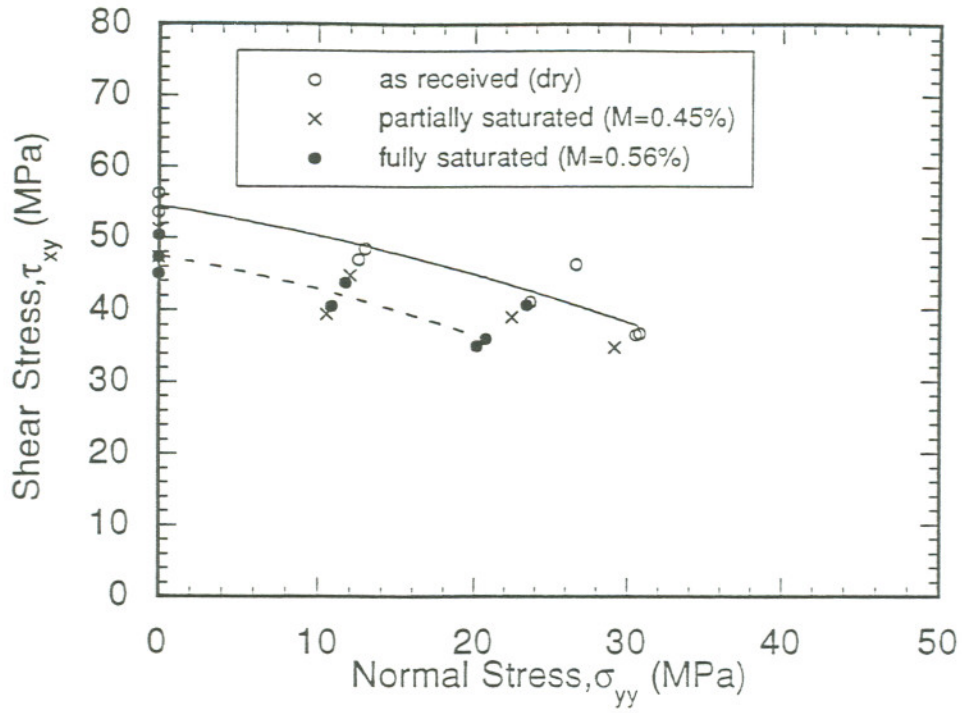


Figure 5-9: Biaxial failure envelope for E-glass/epoxy system

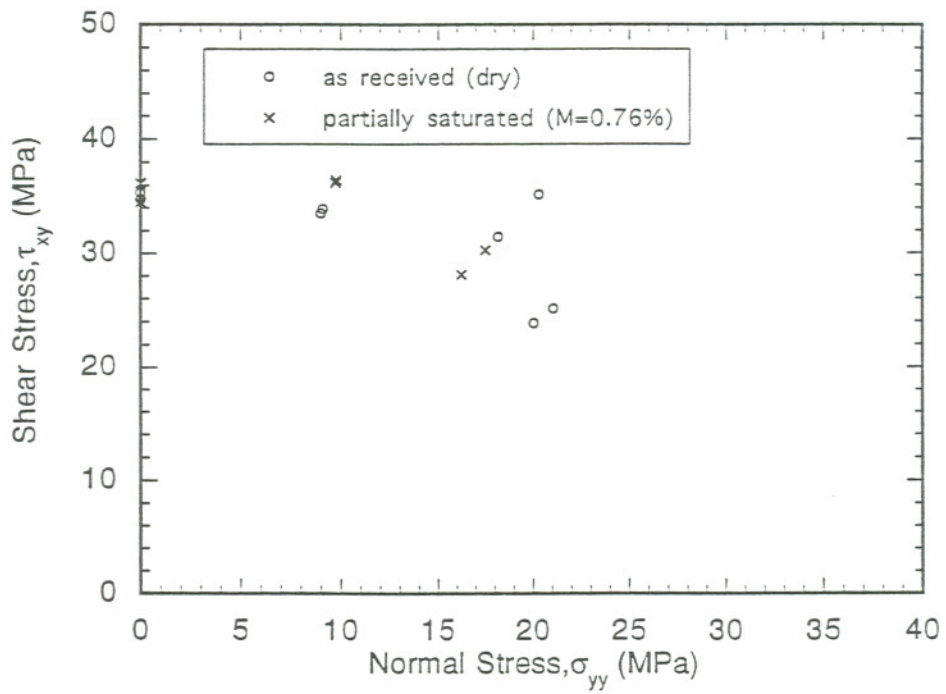


Figure 5-10: Biaxial failure envelope for E-glass/polyester system

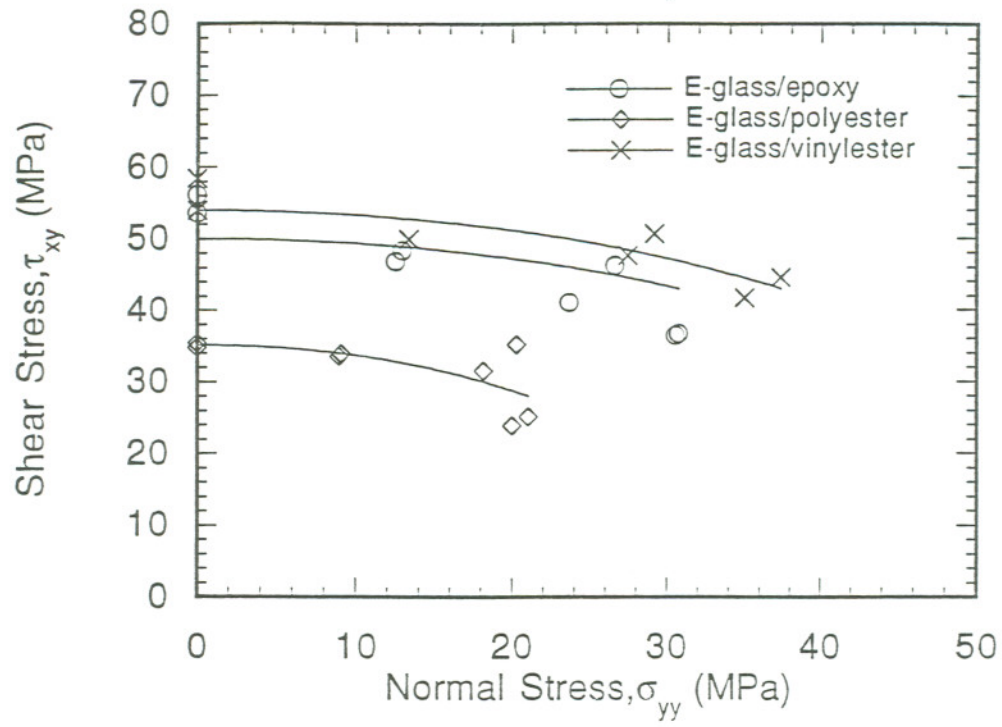


Figure 5-11: Biaxial failure envelope for the E-glass/GRP systems under dry conditions.

Chapter 6

Biaxial Testing of Unidirectional Carbon-epoxy Composite

6.1 Introduction

In this study, the biaxial Iosipescu test fixture has been employed to determine the failure properties of a unidirectional carbon-epoxy composite subjected to combined shear and transverse tensile stresses. The range of possible biaxial stress states has been extended by varying the fiber orientations in the Iosipescu specimens. Results obtained from the shear tests conducted using the biaxial Iosipescu test fixture have been compared with independent Iosipescu tests conducted in the University of Idaho, and the 10° off-axis tension test. It is found that the Iosipescu shear testing of specimens with a fiber angle of 45° can provide reliable estimates for the transverse tensile strength of the material. Using this approach, the biaxial failure properties have been derived in the complete range of shear-transverse tension stress space.

6.2 Experimental Procedure

A series of biaxial Iosipescu, 10° off-axis, and transverse tensile tests were performed. The estimated shear strength values from the Iosipescu specimens were verified by testing the same material using the 10° off-axis tension test and by testing the material in an Iosipescu test fixture based on the Wyoming design [57]. The material tested in this study was a unidirectional carbon-epoxy (XAS-914 from Ciba-Geigy) composite. The following experimental scheme was adopted;

1. Shear testing of 0° - Iosipescu specimens using biaxial Iosipescu test fixture at $\alpha = 0^\circ$ loading angle. Additional shear tests using the shear fixture from University of Idaho for comparison.

2. Shear strength measurements using the 10° off-axis tensile test.

3. Biaxial testing by varying the loading angle from 0° to -30° in the biaxial Iosipescu test fixture using 0° - Iosipescu specimens ($\varphi = 0^\circ$).

4. Shear testing in the biaxial Iosipescu test fixture by varying the fiber angle from 0° to 90° at $\alpha = 0^\circ$ angle.

5. Transverse tensile experiments.

The 0° and the off-axis specimens for the biaxial Iosipescu tests had a length of 80 mm, a width of 20 mm, and a notch depth of 4 mm. The 0° Iosipescu specimens tested in the Idaho fixture had a length of 76.2 mm, a width of 19.05 mm and a notch depth of 5.02 mm. All the specimens had a thickness of 5.08 mm, a notch angle of 90° and a root radius of 0.45 mm.

The 10° off-axis test specimens were rectangular coupons with a length of 228.6 mm, width of 12.7 mm and a thickness of 5.08 mm. The transverse tensile specimens had a length of 203.2 mm in, width of 25.4 mm and a thickness of 5.08 mm. Both the transverse tensile and 10° off-axis specimens had steel tabs glued to the gripping sections.

All the specimens were made by cutting initial blanks with dimensions approximately $\cong 2$ mm in excess of the required values using a band saw with a diamond tipped blade. The blanks were subsequently ground to the final dimensions using a surface grinder. All the machining operations were performed under copious flow of water. Special precautions were taken in machining the notches in the Iosipescu specimens based on the recommendations in reference [58]. The notches were machined to the desired depths using a grinding wheel dressed in the form a V-notch, with an included angle of

90°.

The 0° Iosipescu specimens were tested at loading angles in the range of $0^\circ \leq \alpha \leq -30^\circ$ under shear and shear-transverse tension loading conditions. The off-axis Iosipescu specimens were tested at 0° loading angle with fiber angles in the range of $0^\circ \leq \phi \leq 90^\circ$. Five specimens were tested under pure shear loading of 0° Iosipescu specimens and a minimum of two specimens were tested under other loading conditions. A set of five 0° Iosipescu specimens were tested at the University of Idaho, using the Idaho fixture [57]. In addition, seven 10° off-axis tests and three transverse tensile tests were conducted. All of the above tests were performed at a cross-head displacement rate of 1.5 mm/min (0.001 in/s).

6.3 Experimental Results

6.3.1 Mechanical Test Results

The failure modes observed for the tested specimens are schematically illustrated in Figure 6-1. For all loading angles ($0^\circ \geq \alpha \geq -30^\circ$), the 0° -Iosipescu specimens failed by axial splitting at the roots of the notches (see Figure 6-2), with associated load drops in the load-displacement curve. As has been reported earlier [2,19,20,36], the splits propagated along the fibers and were eventually arrested away from the inner loading points, resulting in the specimen sustaining further loads till ultimate failure. The same kind of failure mode was observed in the 15° off-axis Iosipescu specimens loaded in pure shear. In specimens with larger off-axis angles ($15^\circ < \phi < 90^\circ$), the splits propagated instantaneously along the fibers, resulting in catastrophic failure into three pieces. The 90° -Iosipescu specimens failed at loads lower than the 0° specimens. All the three 90° spec-

imens tested in this study failed along the notch root axis, with additional cracking along the fibers near one of the inner loading points. The 10° off-axis specimens and transverse tensile specimens failed into two pieces by splitting along the fibers.

Failure loads for the 0° and 15° Iosipescu specimens were estimated from the average load for the formation of the two axial splits, while for specimens with fiber angles larger than 15° , failure loads were determined from the load corresponding to catastrophic failure. The maximum load was treated as the failure load for transverse and 10° off-axis tension tests. The results from the various tests are summarized in Tables. 6-1 – 6-6.

The variation of failure loads, from tests performed on 0° -Iosipescu specimens with different loading angles (α), and from the off-axis Iosipescu specimens with different fiber angles (ϕ), is presented in Figures 6-3 and 6-4 respectively. From Figure. 6-3, it appears that the average loads for the formation of the axial splits decrease with decreasing loading angles for the 0° specimens. For tests performed on off-axis specimens, the failure loads decrease with increasing fiber angles up to 45° and then increase with further increase in the fiber angle (see Figure 6-4).

6.3.2 Fractography

The morphology of the fracture surfaces can be expected to establish possible differences in the modes of failure. In polymeric matrix composites, transverse tensile failure exhibits a plane fracture surface with bare fiber surfaces [59]. On the other hand, shear failure exhibits a relatively rough fracture surface, with extensive surface lacerations in the matrix [59]. A topographical feature called a cusp or hackle observable in the matrix region, is also associated with shear failure of the composite [60,61].

In this study, a qualitative examination of the fracture surfaces of the failed specimens was performed by using scanning electron microscopy (SEM). The surfaces were coated with Gold-Palladium and were imaged in the secondary electron emission mode. The SEM analyses were performed for Iosipescu specimens with fiber angles of 0° , 45° , and 90° . In addition, the fracture surfaces from the 10° off-axis tension and transverse tension specimens were also observed. Representative fracture morphologies seen on the various specimens are shown in Figures. 6-5 – 6-9. In general, all fracture surfaces appear to be similar, with the exception of the transverse tensile specimens. A closer examination of these surfaces reveals the following;

1) In the 0° Iosipescu specimens tested at $\alpha = 0^\circ$, hackles were observed in regions close to the notch roots. The fiber surfaces were covered with fragments of the matrix, indicating that the fracture process occurred either close to the interface or within the matrix. In regions away from the notch roots, hackles as well as bare fibers were observed, indicating that the fracture process initiated in shear and propagated under biaxial stress conditions.

2) The 90° Iosipescu specimens tested at $\alpha = 0^\circ$ exhibited hackles and rough fiber surfaces. The extent of bare fiber regions were relatively smaller compared to that of the 0° specimens. This indicates that the fracture process propagated in a predominantly shear mode.

3) Both hackled and bare fiber regions were observed in the 10° off-axis tension specimens. The extent of hackled regions was not significantly different between the edges and the interior of the specimen.

4) In the transverse tensile specimens, the entire fracture surface had predominantly bare fibers. Some hackles were seen in the matrix regions between the fibers. However, these hackles looked significantly different in comparison with the shear tested specimens. They appeared more like serrations instead of the characteristic elongated S-shaped hackles seen in the shear tested specimens.

5) Similar to the transverse tensile specimens, the 45° off-axis Iosipescu specimens tested at $\alpha = 0^\circ$ exhibited a smooth fracture surface, with very few hackled regions.

In summary, it appears that the failures in the 0° and 90° Iosipescu specimens tested at $\alpha = 0^\circ$, and the 10° off-axis tension specimens, initiated in a predominantly shear mode. On the other hand, the transverse tensile and 45° off-axis Iosipescu specimens tested at $\alpha = 0^\circ$ failed in a predominantly tensile mode.

6.4 Discussion

In this study, a series of shear and biaxial Iosipescu tests were conducted on a unidirectional carbon-epoxy composite by varying the loading angles. In addition, off-axis Iosipescu tests were also performed in order to extend the range of biaxial stress states achievable in the biaxial Iosipescu test (BIT) fixture. To further verify the shear test results from the BIT, additional shear tests were performed by using the Idaho fixture and 10° off-axis tension tests. Furthermore, fracture morphologies of some of the tested specimens were qualitatively examined.

Figures 6-10 and 6-11 show that the average shear strength values, estimated from the three different shear test methods employed in this study, are in good agreement. It should however be noted that the shear strength for the 0° Iosipescu specimens was estimated from the loads at failure divided by the cross sectional area. This approach assumes that the shear stress distribution is constant along the notch root axis. Broughton [2,20] and Bansal et.al [36] have used the same approach for determining the biaxial strength properties of unidirectional composites using the Iosipescu test method. It is interesting to note that the number of valid results achieved from the 10° off-axis tension tests is less than 50% of the total number of tested specimens, since most specimens failed at the grips

at relatively low loads. However, almost all of the Iosipescu specimens tested in both the BIT fixture, and the Idaho fixture gave fairly consistent strength values.

For the off-axis Iosipescu specimens, the failure loads decreased for fiber angles from 0° to 45° , and increased for fiber angles from 45° to 90° (see Figure 6-4). Once again, assuming that the stresses at the notch roots in the off-axis Iosipescu specimens are identical to the specimen center, the observed trend in the failure loads can be explained from the average stress distributions shown in Figures 3-2 and 3-3. The transverse tensile stresses (see Figure 3-2) increase for fiber angles in the range $0^\circ \leq \varphi \leq 45^\circ$, and decrease for fiber angles in the range $45^\circ \leq \varphi \leq 90^\circ$. Furthermore, since a change in sign of the average shear stress in the material directions will not affect the mode of failure [6], it can be seen from Figure 3-3 that the absolute value of the shear stress decreases for fiber angles from 0° to 45° , and increases for fiber angles from 45° to 90° . In addition, since the in-plane shear strength for this composite is expected to be larger than the transverse tensile strength, one can expect the failure loads to decrease from $\varphi = 0^\circ$ to 45° , and increase symmetrically from $\varphi = 45^\circ$ to 90° . However, as can be seen in Figure 6-4, lower failure loads were observed for fiber angles $\varphi > 45^\circ$. This is most likely due to the fact that the microdamage at the notch roots, or within the material, might have a more severe effect for specimens with fiber angles $\varphi > 45^\circ$. Figures 3-2 and 3-3 also show that the average stress state in the gage section of 45° -Iosipescu specimens, loaded at $\alpha = 0^\circ$, will be tensile in the direction perpendicular to the fibers, with an equal component of compressive stresses along the fibers. Using equations 3-1, 3-2 and 3-3, the average transverse tensile stress at failure of these specimens was calculated to be 38 MPa. This result is in excellent agreement with the transverse tensile strength of 39 MPa obtained from the uniaxial transverse tension tests, thus implying that the 45° -Iosipescu specimens failed due to transverse tension, with an insignificant effect of the longitudinal compressive stresses on the final failure. The shear loading of 45° off-axis Iosipescu

specimens could be considered to be equivalent to applying a torsional load to tubes with fibers oriented at -45° to the hoop direction. Such tests [62] have also revealed that the material fails essentially in a transverse tensile mode.

The failure loads obtained from the biaxial Iosipescu tests performed at different loading angles (α) and fiber orientations (ϕ), in conjunction with equations 3-1, 3-2, and 3-3, can be used to estimate the average biaxial stresses within the specimen gage section at the onset of failure. Using this approach, a biaxial failure envelope is presented in Figure 6-12. It can be noticed that the experimental points cover the entire region of the shear-transverse tension stress space, and are in good agreement with the Tsai-Hill criterion for biaxial failure of unidirectional composites [63]. Since the strength of the material in the fiber direction (σ_{xx}^f) is much higher in comparison with the in-plane shear strength (σ_{xy}^f) and the transverse tensile strength (σ_{yy}^f), a modified Tsai-Hill failure criterion [63] was used in Figure 6-12.

$$\left(\frac{\sigma_{xy}}{\sigma_{xy}^f}\right)^2 + \left(\frac{\sigma_{yy}}{\sigma_{yy}^f}\right)^2 = 1 \quad (4)$$

The analytical expressions (equations 3-1 and 3-2) that were used to estimate the shear and normal stresses assume a uniform stress distribution along the notch root axis. However, finite element analyses of the Iosipescu specimen by various researchers [1,7,16,17,20,21,23,27,36,64-66] have indicated that this assumption is not valid in linear elastic media. For a 0° specimen loaded in pure shear, the actual shear stress at the specimen center is found to be lower than the average value predicted by equation (2), with stress concentrations occurring in the vicinity of the notch roots. The extent of stress concentration seems to increase not only with increasing orthotropy ratios of the specimen, but also with a decreasing element size at the notch roots [36]. This implies that the

stress field at the notch tips is either highly concentrated, or singular in nature for the case of a perfectly sharp notch [27]. On the other hand, nonlinear finite element analyses performed [29] for 0° graphite-epoxy specimens have indicated that the shear stress concentration decreases with increasing load values, whereas the strains remain concentrated at the notch roots. The decrease in the shear stress concentration can be expected as a result of matrix yielding. Therefore, it seems reasonable to assume that the actual stress at the notch root approaches the average stress within the gage section at the onset of failure. Although this approach is too simplistic in nature, the results are fairly consistent barring the fact that composite materials, in general, show a wide scatter for strength values owing to their inherent inhomogeneity. Further, in this analysis, failure has been treated as the formation of axial splits in spite of the fact that the 0° specimens continue to withstand larger loads until final fracture occurs with appreciable crushing at the inner loading points. However, the loads for the formation of axial splits can be considered as a conservative estimate of the shear or biaxial intralaminar failure load, since the exact partitioning of stresses at final fracture can only be determined from a solution which takes into account the location of the loading points, the friction between the specimen and the loading points, and the non-linear material behavior due to damage accumulation.

From the tests performed in this study, the microscopic shear failure of the composite needs to be addressed. The rough fracture surfaces, as observed in the Iosipescu and off-axis specimens, with the formation of hackles indicates that the fracture process is much more complex at the microscopic level. The formation of hackles has been attributed to the localized tensile mode of failure in the matrix [67]. Without a complete understanding of the development of the micro-damage within the material, the measured strength values can be viewed as the resistance of the material to macroscopic shear loading.

The results obtained in this study indicate that the biaxial Iosipescu test, with variations in the loading angle as well as the specimen fiber orientation, can provide a simple

methodology for characterizing the shear and biaxial failure properties of unidirectional composite materials.

6.5 Conclusions

Based on the test results, the following conclusions can be drawn.

1. The biaxial Iosipescu fixture can provide consistent values for the shear strength of the tested material. The measured strength value, treating the average load for the formation of axial splits as failure, compares well with the 10° off-axis tension test and the Iosipescu shear test performed in the Idaho fixture.

2. The shear loading of 45° off-axis Iosipescu specimens provide reliable estimates for the transverse tensile strength of the tested unidirectional carbon-epoxy composite, as indicated by the strength values measured from the transverse tensile tests.

3. Biaxial Iosipescu tests performed by varying the loading angle and the fiber angle can be used to generate a complete failure envelope for the shear-transverse tensile stress space. The test results indicate that this procedure yields fairly accurate results for the biaxial failure envelope of carbon-epoxy composites.

Table 6-1: Shear Test Results (using Biaxial Iosipescu Test Fixture)

Specimen No	Loading Angle, deg	Fiber Angle, deg	Avg. load for splitting, kN	Shear stress at failure, MPa
1	0°	0°	4.759	78.08
2	0°	0°	4.937	81.00
3	0°	0°	4.292	70.42
4	0°	0°	4.826	79.18
5	0°	0°	4.893	80.27

cross sectional area: 12.00 mm X 5.08 mm

specimen type: 0° -specimens

Table 6-2: Shear Test Results (using Idaho Test Fixture)

Specimen No	Loading Angle, deg	Fiber Angle, deg	Avg. load for splitting, kN	Shear stress at failure, MPa
1	0°	0°	3.452	75.36
2	0°	0°	2.931	64.00
3	0°	0°	3.247	70.89
4	0°	0°	3.269	71.38
5	0°	0°	3.690	80.56

cross sectional area: 9.02 mm X 5.08 mm

specimen type: 0° -specimens

Table 6-3: 10° Off Axis Test Results

Specimen No	Failure Load, kN	Shear stress at failure, MPa	Remarks
1	25.79	71.62	
2	28.58	79.38	
3*	24.83	73.22	failure in the gage section
4**	22.92	69.49	
5	22.85	63.47	
6	24.14	67.05	failure in the grip section
7	20.31	56.40	

cross sectional area: 12.70 mm X 5.08 mm

*cross sectional area: 11.96 mm X 5.08 mm

**cross sectional area: 11.63 mm X 5.08 mm

fiber angle: 10.5°

Table 6-4: Biaxial Iosipescu Test Results (with loading angle variation)[†]

Specimen No	Loading Angle, deg	Avg. load for splitting, kN	Shear stress at failure, MPa	Normal stress at failure, MPa	Remarks
1	0°	4.759	78.08	0.00	pure shear tests.
2	0°	4.937	81.00	0.00	
3	0°	4.292	70.42	0.00	
4	0°	4.826	79.18	0.00	
5	0°	4.893	80.27	0.00	
6	5°	4.759	77.78	6.81	shear-transverse tension tests
7	5°	4.715	77.06	6.74	
8	10°	4.372	70.642	12.46	
9	10°	4.492	72.58	12.80	
10	10°	4.706	76.03	13.41	
11	15°	4.782	75.77	20.30	
12	15°	4.226	66.96	17.94	
13	20°	4.626	71.31	25.96	
14	20°	4.461	68.78	25.03	
15	20°	4.203	64.80	23.59	
16	30°	4.150	58.96	34.04	
17	30°	4.648	66.04	38.13	
18	30°	4.203	59.72	34.47	
19	30°	4.070	57.82	33.39	

Table 6-5: Off-axis Iosipescu Test Results^{††}

Specimen No	Fiber Angle, deg	Avg splitting load, kN	Shear stress at failure, MPa	Normal stress at failure, MPa	Remarks
1	15°	3.683	52.33	30.21	specimen failed by splitting
2	15°	3.683	52.33	30.21	
3	30°	2.402	19.70	34.13	catastrophic failure
4	30°	2.446	20.07	34.76	
5	35°	2.402	13.48	37.03	
6	35°	2.847	15.97	43.89	
7	40°	2.558	7.29	41.32	
8	40°	2.224	6.33	35.93	
9	45°	2.291	0.00	37.58	
10	45°	2.068	0.00	33.93	
11	45°	2.180	0.00	35.76	
12	45°	2.424	0.00	39.77	
13	50°	2.135	6.08	34.49	
14	50°	1.824	5.20	29.46	
15	60°	1.957	16.05	27.81	
16	60°	2.268	18.61	32.23	
17	75°	2.936	41.71	24.08	
18	75°	3.025	42.97	24.81	
19	90°	3.647	59.89	0.00	

Table 6-5: Off-axis Iosipescu Test Results^{††}

Specimen No	Fiber Angle, deg	Avg splitting load, kN	Shear stress at failure, MPa	Normal stress at failure, MPa	Remarks
20	90°	2.268	37.25	0.00	catastrophic failure
21	90°	2.491	40.90	0.00	

[†]cross sectional area: 12.00 mm X 5.08 mm; specimen type: 0° -specimens

^{††}cross sectional area: 12.00 mm X 5.08 mm; loading angle: 0°

Table 6-6: Transverse Tensile Test Results

Specimen No	Failure Load, kN	Stress at failure, MPa	Remarks
1 ^a	3.687	38.09	failure in the gage section
2 ^b	4.777	37.72	
3 ^b	3.732	28.91	failure near the grip section

^a cross sectional area: 19.05 mm X 5.08 mm; dog bone specimen

^b cross sectional area: 25.4 mm X 5.08 mm; rectangular coupons

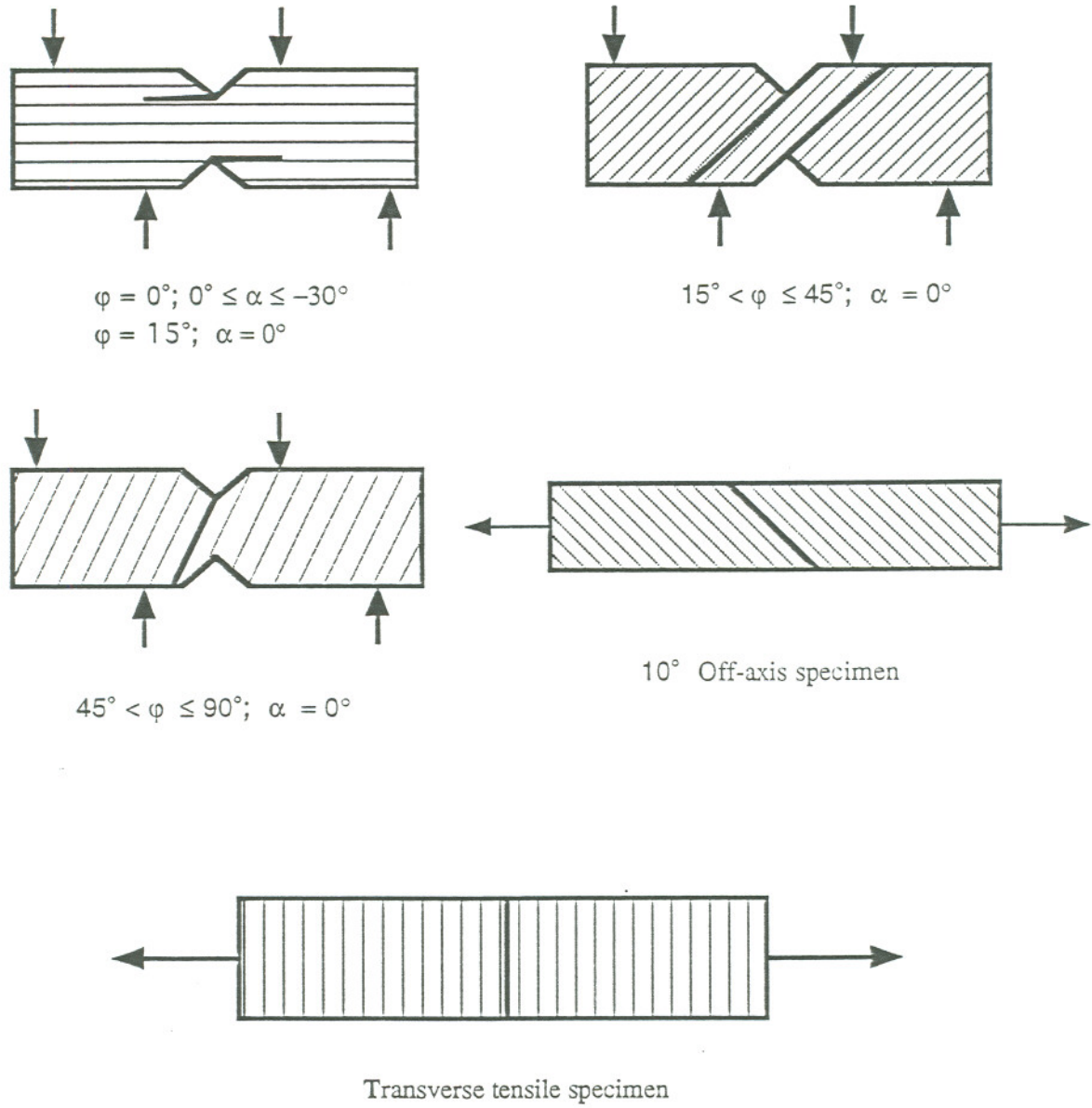


Figure 6-1: Schematic illustration of the observed failure modes in the various tests.

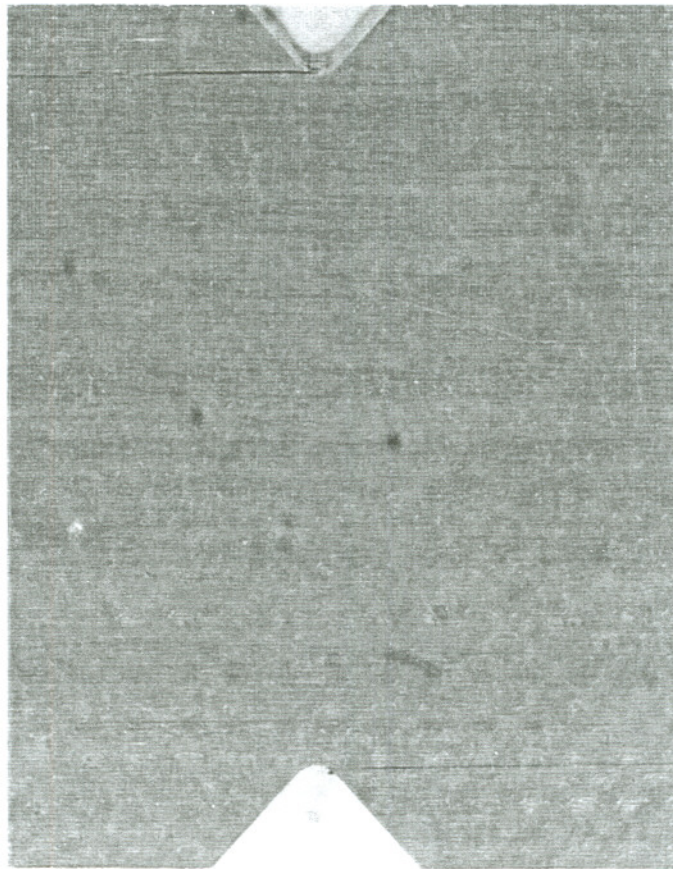


Figure 6-2: Photo-micrograph of the axial splits in the 0° Iosipescu specimens.

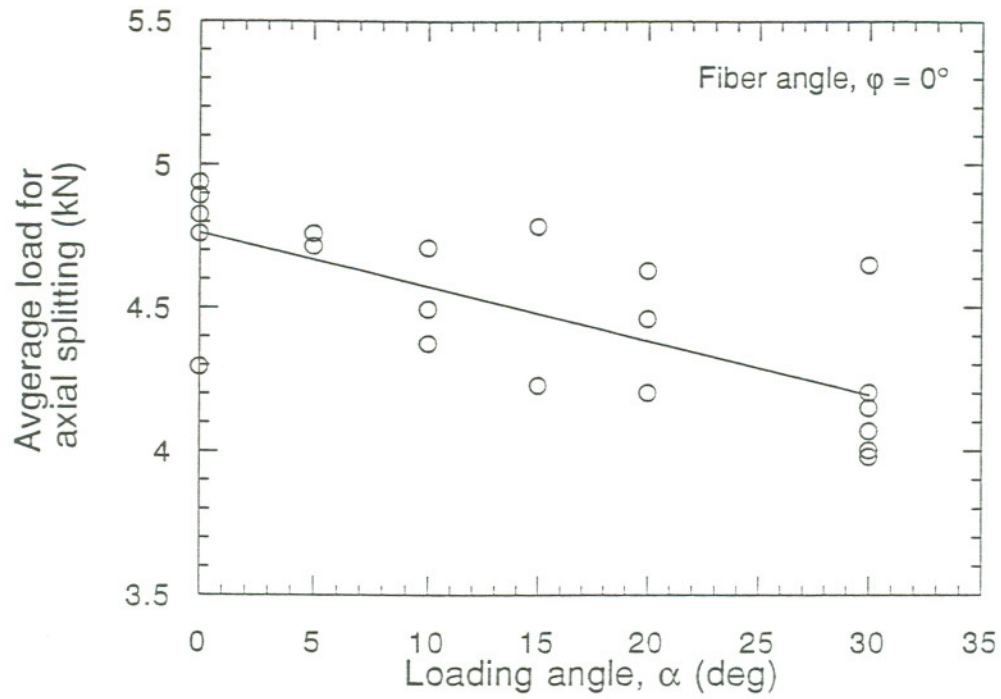


Figure 6-3: Failure loads for the tested specimens as a function of the loading angle.

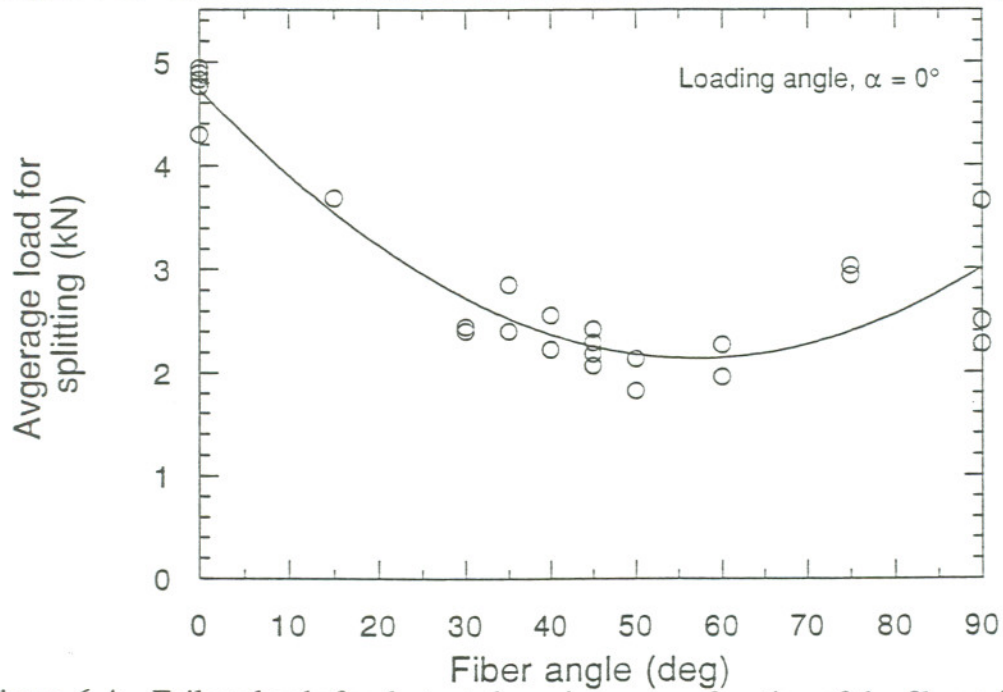


Figure 6-4: Failure loads for the tested specimens as a function of the fiber orientation.

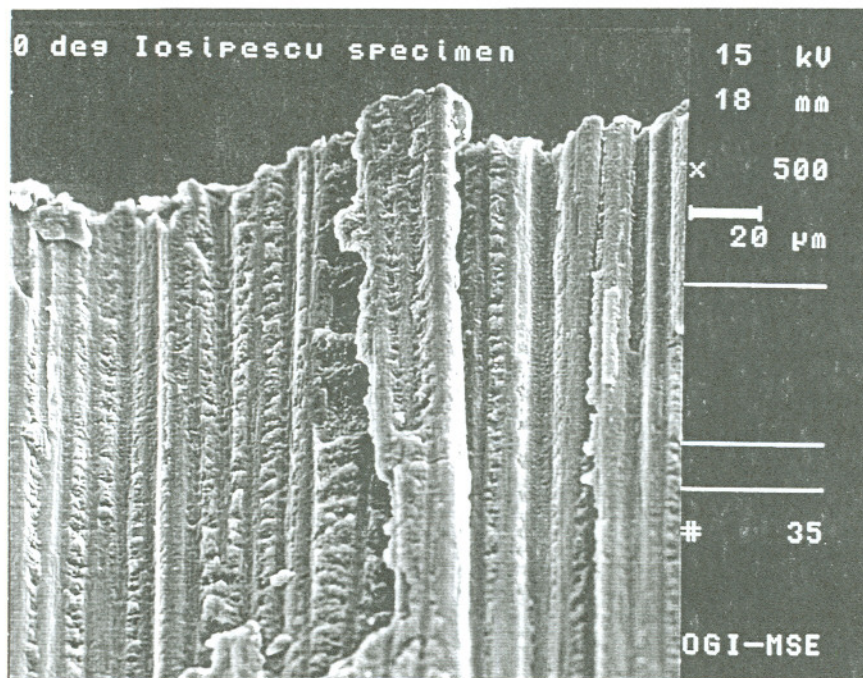


Figure 6-5: Fracture surface morphology of the Iosipescu specimen tested at $\alpha = 0^\circ$ and $\varphi = 0^\circ$.

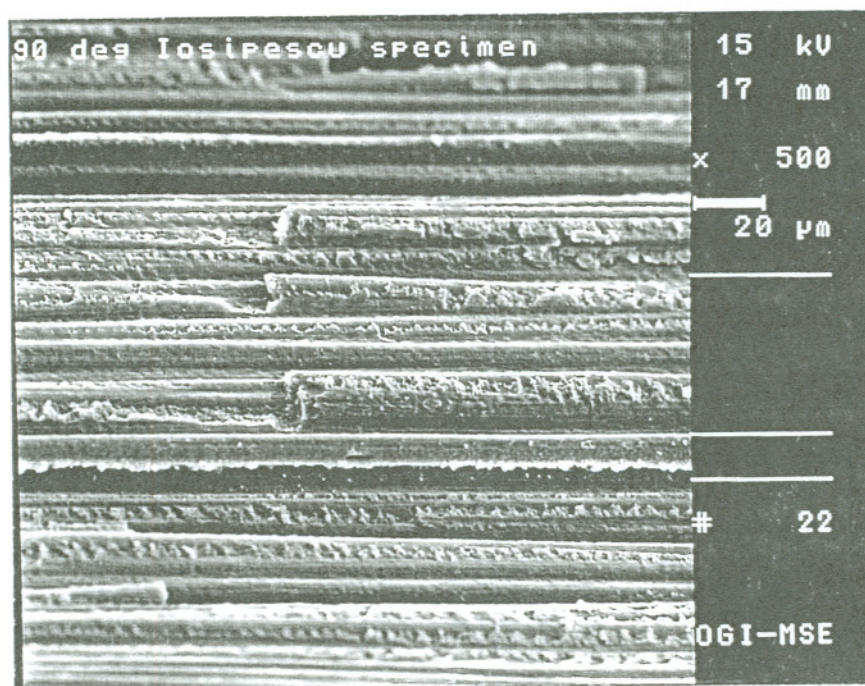


Figure 6-6: Fracture surface morphology of the Iosipescu specimen tested at $\alpha = 0^\circ$ and $\varphi = 90^\circ$.

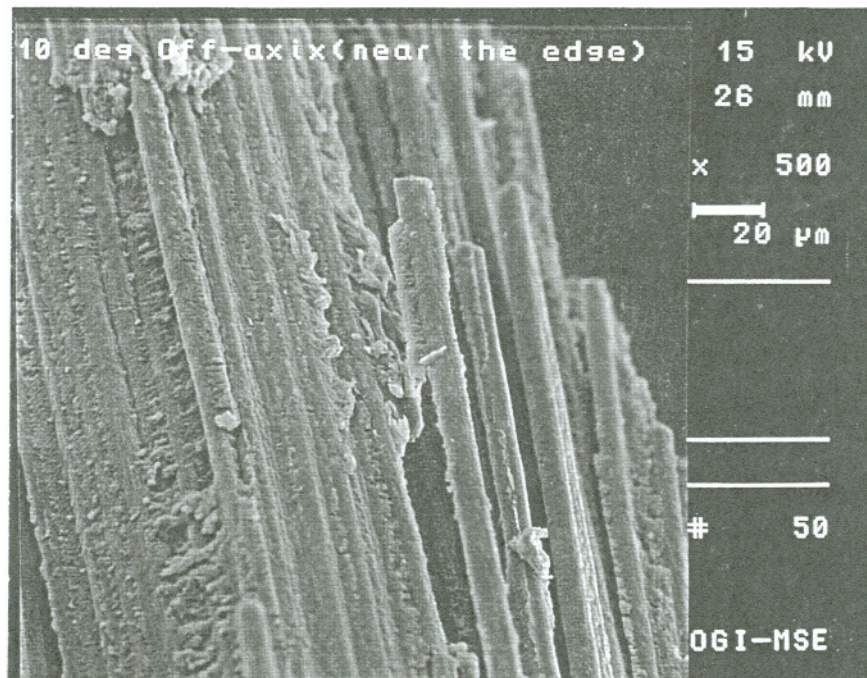


Figure 6-7: Fracture surface morphology of the 10° off-axis specimen.

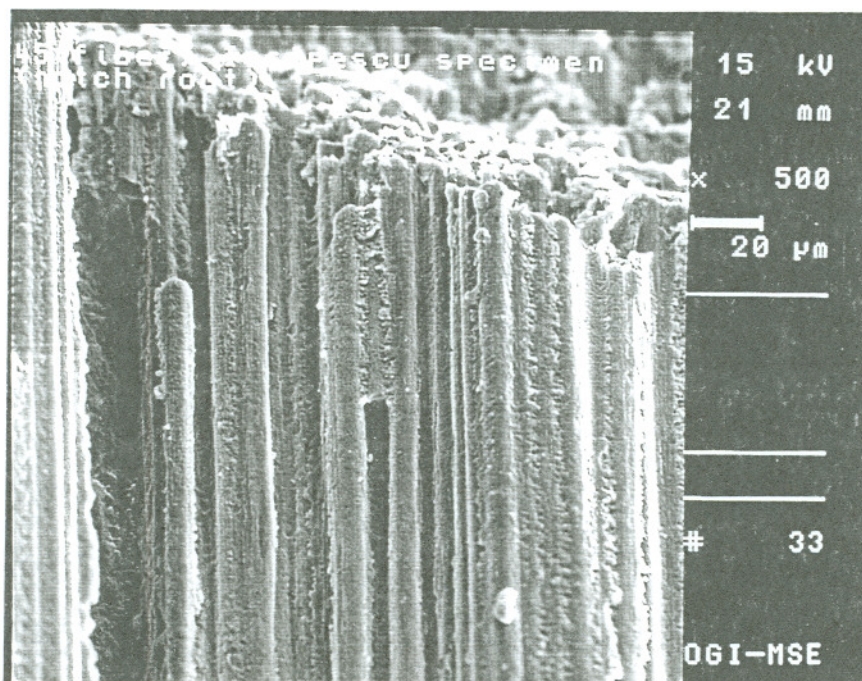


Figure 6-8: Fracture surface morphology of the Iosipescu specimen tested at $\alpha = 0^\circ$ and $\varphi = 45^\circ$.

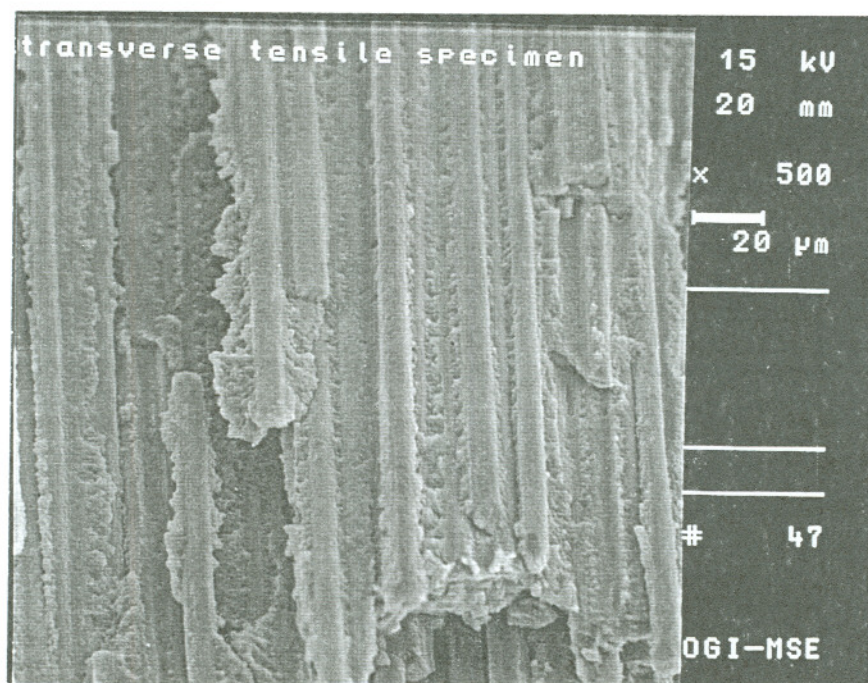


Figure 6-9: Fracture surface morphology of the tested transverse tensile specimen.

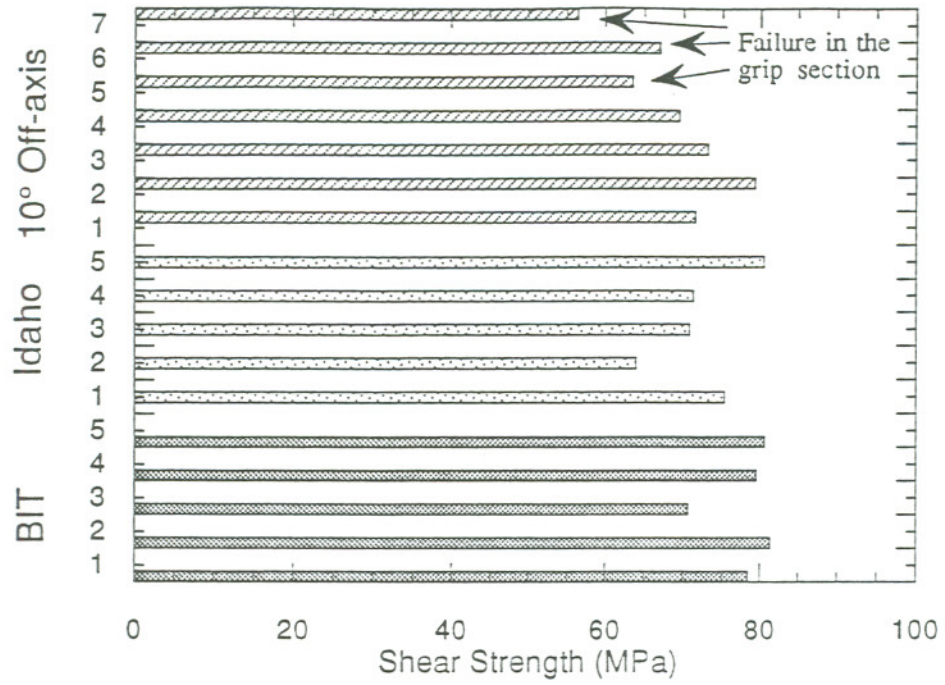


Figure 6-10: Shear test results from the employed test methods.

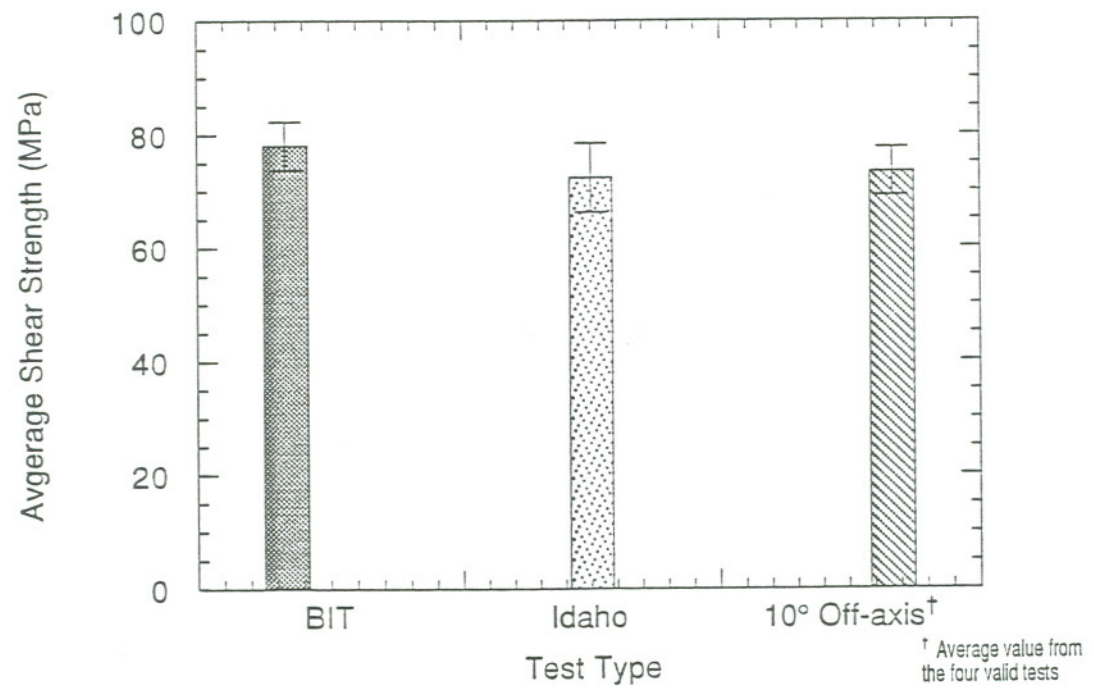


Figure 6-11: Comparison of the estimated average shear strengths from the various tests.

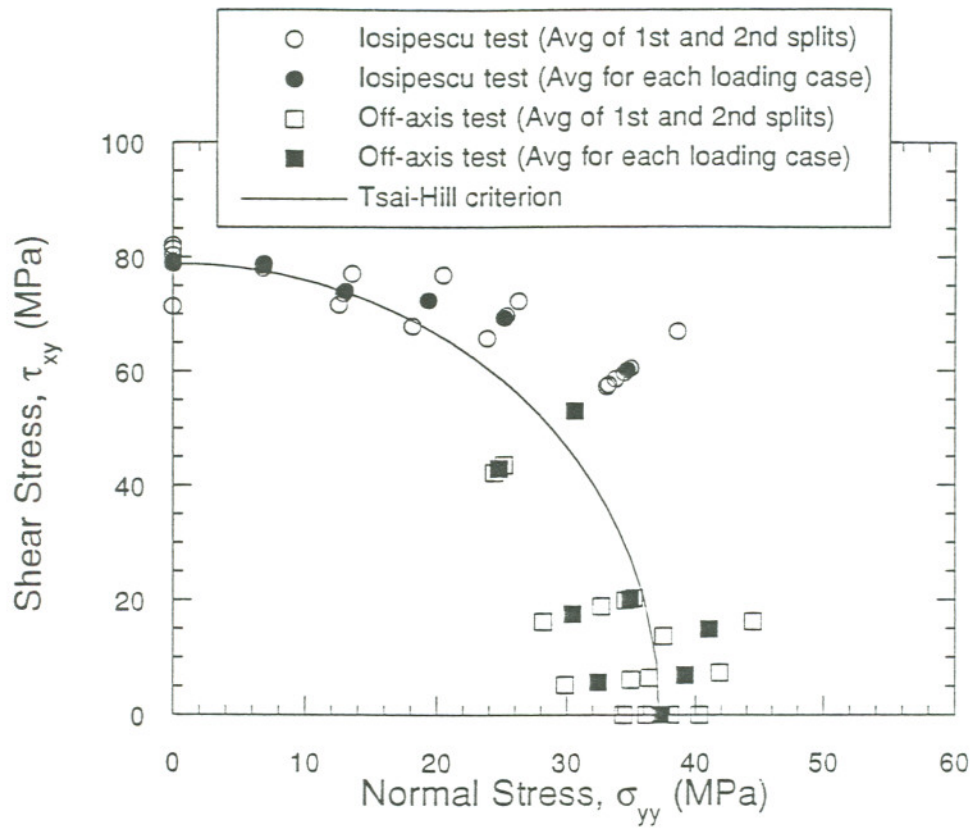


Figure 6-12: Normal versus shear stress at failure for the biaxial tests performed.

Chapter 7

Conclusions

The results from this work may be summarized as follows

- (1) This work has shown that the modified biaxial test fixture could be used effectively for shear property measurements and biaxial failure envelope generation for unidirectional composite materials. With regard to cyclic testing, though the fixture has limited capabilities, it can still be used for generating a fatigue failure surface.
- (2) From the mechanical tests performed on E-glass/GRP systems, the following conclusions can be drawn. E-glass/polyester system showed the lowest resistance to axial splitting, while the glass vinylester system showed highest resistance to axial splitting. The fully saturated glass/epoxy system failed at significantly lower loads compared to that of the dry specimens. The reduction in the failure loads was approximately 10 - 15%. In the partially saturated glass/polyester and glass/vinylester systems no significant effect of absorbed moisture on the failure properties was observed
- (3) From the tests performed on the carbon/epoxy composite, it can be concluded that the fixture can provide consistent values for the shear strength of the tested material. The measured strength value, treating the average load for the formation of axial splits as failure, compares well with the 10° off-axis tension test and the Iosipescu shear test performed in the Idaho fixture.
- (4) The shear loading of 45° off-axis Iosipescu specimens provide reliable estimates for the transverse tensile strength of the tested unidirectional carbon-epoxy composite, as indicated by the strength values measured from the trans-

verse tensile tests.

- (5) Biaxial Iosipescu tests performed by varying the loading angle and the fiber angle can be used to generate a complete failure envelope for the shear-transverse tensile stress space. The test results indicate that this procedure yields fairly accurate results for the biaxial failure envelope of carbon-epoxy composites.

References

1. Pindera, M-J., "Shear testing of Fiber reinforced metal Matrix Composites," *Metal Matrix Composites: Testing, Analysis and Failure Modes*, W. S. Johnson, Editor., ASTM:STP 1032, pp. 19-42, Philadelphia, PA (1989)
2. Broughton, W. R., *Shear Properties of Unidirectional Carbon Fibre Composites*, Ph.D. Thesis, University of Cambridge, Cambridge, U.K. (1989)
3. Daniel, I.M., "Testing, Mechanical Characterization," *International Encyclopedia of Composites*, S. M. Lee, Editor., VCH Publishers, Inc., pp. 436-464, New York (1991)
4. Found, M.S., "A Review of the Multiaxial Fatigue Testing of Fiber Reinforced Plastics," *Multiaxial Fatigue*, ASTM STP 853, K. J. Miller and M. W. Brown, Editors. ASTM, pp. 381-395, Philadelphia (1985)
5. Sun, C.T., Chen, J.L., Sha, G.T., and Koop, W.E., "Mechanical Characterization of SCS-6/Ti-6-4 Metal Matrix Composite," *Journal of Composite Materials* vol. **24**, pp. 1029-1059, (1990)
6. Jones, R. M., *Mechanics of Composite Materials*, McGraw-Hill, (1975)
7. Pindera, M-J., Choksi, G., Hidde, J.S., and Herakovich, C.T., "A Methodology for Accurate Shear Characterization of Unidirectional Composites," *Journal of Composite Materials* vol. **21**, pp. 1164-1183, (1987)
8. Chamis, C.C. and Sinclair, J.H., "Ten-degree Off-axis Test for Shear Properties in Fiber Composites," *Experimental Mechanics* vol. **17(9)**, pp. 339-346, (1977)
9. Pindera, M-J. and Herakovich, C.T., "Shear Characterization of Unidirectional Composites with the Off-Axis Tension Test," *Experimental Mechanics* vol. **26(1)**, pp. 103-112, (1986)
10. Iosipescu, N., "New Accurate Procedure for Single Shear Testing of Metals," *Journal of Materials* vol. **2**, pp. 537-566, (1967)

11. Arcan, M., Hashin, Z., and Voloshin, A., "A Method to Produce Uniform Plane-Stress States with Applications to Fiber-reinforced Materials," *Experimental Mechanics* vol. **18(4)**, pp. 141-146, (1978)
12. Voloshin, A. and Arcan, M., "Failure of Unidirectional Fiber-reinforced Materials-New Methodology and Results," *Experimental Mechanics* vol. **20(8)**, pp. 280-284, (1980)
13. Spigel, B.S., Prabhakaran, R., and Sawyer, J.W., "An Investigation of the Iosipescu and Asymmetrical Four-Point Bend Tests," *Experimental Mechanics* vol. **27**, pp. 57-63, (1987)
14. Walrath, D.E. and Adams, D.F., "The Iosipescu Shear Test as Applied to Composite Materials," *Experimental Mechanics* vol. **23**, pp. 105-110, (1983)
15. Adams, D.F. and Walrath, D.E., "Iosipescu Shear Properties of SMC Composite Materials," *Composite Materials: Testing and Design (Sixth Conference)*, I. M. Daniel, Editor., ASTM (STP 787), pp. 19-33, (1982)
16. Walrath, D.E. and Adams, D.F., "Verification and Application of the Iosipescu shear test method," *Department Report UWME-DR-401-103-1*, Mechanical Engineering Department, University of Wyoming, Laramie, Wyoming 82071, USA (1984)
17. Walrath, D.E. and Adams, D.F., "Analysis of Stress State in an Iosipescu Shear Test Specimen," *Department Report UWME-DR-301-102-1*, Mechanical Engineering Department, University of Wyoming, Laramie, Wyoming 82071, USA (1983)
18. Adams, D.F. and Walrath, D.E., "Iosipescu Shear Properties of SMC Composite Materials," *Composite Materials: Testing and Design (Sixth Conference)*, ASTM STP 787, pp. 19-33, (1992)
19. Adams, D.F. and Walrath, D.E., "Further Development of the Iosipescu Shear Test Method," *Experimental Mechanics* vol. **27(2)**, pp. 113-119, (1987)
20. Broughton, W.R., Kumosa, M., and Hull, D., "Analysis of the Iosipescu Shear Test as Applied to Unidirectional Carbon-fiber reinforced Composites," *Composites Science and Technology* vol. **38**, pp. 299-325, (1990)
21. Ho, H., Tsai, M.Y., Morton, J., and Farley, G.L., "An Experimental Investigation of Iosipescu Specimen for Composite Materials," *Experimental Mechanics* vol. **31(4)**, pp. 328-336, (1991)

22. Sullivan, J.L., Kao, B.G., and Van Oene, H., "Shear Properties and a Stress Analysis Obtained from Vinyl-ester Iosipescu Specimens," *Experimental Mechanics* vol. **24**(3), pp. 223-232, (1984)
23. Morton, J., Ho, H., Tsai, M.Y., and Farley, G.L., "An Evaluation of the Iosipescu Specimen for Composite Materials Shear Property Measurement," *Journal of Composite Materials* vol. **26**, pp. 708-750, (1992)
24. Bretz, G.T., Houston, D.Q., Sullivan, J.L., Hagerman, E., and Kakarala, N., "Discussion of Test Procedures Involving Iosipescu Shear Testing," *Advanced Composites: Design, Materials and Processing Technologies*, ASM International, pp. 299-307, Materials Park, OHIO (1992)
25. Dearlove, T., Hagerman, E., Kakarala, N., Denton, D., Peterson, D., Lynn, J., Bretz, G.T., Johnson, C., and Melotik, D., *ACC Test Procedures Manual* (ACCM-T-001), (1990)
26. Abdallah, M.G. and Gascoigne, H.E., "The Influence of Test Fixture Design on the Iosipescu Shear Test for Fiber Composite Materials," *Test Methods for Design Allowables for Fibrous Composites: 2nd Volume*, ASTM STP 1003, C. C. Chamis, Editor., American Society for Testing and Materials, pp. 231-260, Philadelphia (1989)
27. Sukumar, N. and Kumosa, M., "Application of the Finite Element Iterative methods to cracks and sharp notches in orthotropic media," *International Journal of Fracture* vol. **58**, pp. 177-192, (1992)
28. Sukumar, N. and Kumosa, M., "Finite element analysis of axial splits in composite Iosipescu specimens," *International Journal of Fracture* vol. **62**, pp. 55-85, (1993)
29. Ho, H., Morton, J., and Farley, G.L., "Non-linear Numerical Analysis of the Iosipescu Specimen for Composite Materials," *Composites Science and Technology* vol. **50**, pp. 355-365, (1994)
30. Lee, S. and Munro, M., "Evaluation of In-Plane Shear Test Methods for Composite Materials by the Decision Analysis Technique," *Composites* vol. **17**, pp. 13-22, (1986)
31. Clyne, T. W. and Withers, P. J., *An Introduction to Metal Matrix Composites*, Cambridge University Press, Cambridge, U.K. (1993)

32. Adams, D.F. and Walrath, D.E., "Current Status of the Iosipescu Shear Test Method," *Journal of Composite Materials* vol. **21**, pp. 494-507, (1987)
33. Swanson, S.R., Messick, M., and Toombes, G.R., "Comparison of torsion tube and Iosipescu in-plane shear test results for a carbon fibre-reinforced epoxy composite," *Composites* vol. **16(3)**, pp. 220-224, (1985)
34. Bert, C.W., Mayberry, B.L., and Ray, J.O., *Composite Materials Testing and Design*, STP 460, American Society for testing and Materials, pp. 362-380, (1969)
35. Smith, E.W. and Pascoe, K.J., *Proceedings, 2nd International Conference on Mechanical Behavior of Materials*, pp. 941-945, (1976)
36. Bansal, A. and Kumosa, M., "Experimental and Analytical Studies of Failure Modes in Iosipescu Specimens under Biaxial Loadings," *Journal of Composite Materials* vol. **29 (3)**, pp. 334-358, (1995)
37. Bansal, A., Schubert, A., Balakrishnan, M. V., and Kumosa, M., *Analytical and Experimental Studies of Substation NCI's*, Final Report to Bonneville Power Administration, Dept. of Materials Science and Engineering, Oregon Graduate Institute of Science and Technology, P.O. Box 91000, Portland, OR 97291-1000, USA, (1994)
38. Balakrishnan, M. V. and Kumosa, M., *Biaxial Testing of a SiC-Ti Metal Matrix Composite*, Report to GE Aircraft Engines, Dept. of Materials Science and Engineering, Oregon Graduate Institute of Science and Technology, P.O. Box 91000, Portland, OR 97291-1000, USA, (1993)
39. Chawla, K.K., "Fatigue," *International Encyclopedia of Composites*, S. M. Lee, Editor., VCH Publishers, Inc., pp. 107-116, New York (1991)
40. Chawla, K. K., *Metal Matrix Composites: Mechanisms and Properties*, Academic Press, San Diego (1991)
41. Owen, M.J. and Found, M.S., "The fatigue behavior of glass-fabric-reinforced polyester resin under off-axis loading," *Journal of Physics D: Applied Physics* vol. **8**, pp. 480-497, (1975)
42. Reifsnider, K., "Fatigue behavior of composite materials," *International Journal of Fracture* vol. **16**, pp. 563-583, (1980)

43. Chan, K.S. and Davidson, D.L., "Fatigue Crack Growth in Fiber-Reinforced Metal-Matrix Composites," *Fatigue of Advanced Materials*, R. O. Ritchie, R. H. Dauskardt, and B. N. Cox, Editors., MCPE, pp. 325-343, Birmingham UK (1992)
44. Johnson, W.S., "Fatigue of Continuous Fiber Reinforced Titanium Matrix Composites," *Fatigue of Advanced Materials*, R. O. Ritchie, R. H. Dauskardt, and B. N. Cox, Editors., MCPE, pp. 357-377, Birmingham, U.K. (1992)
45. Dvorak, G.J. and Johnson, W.S., "Fatigue of Metal Matrix Composites," *International Journal of Fracture* vol. **16**, pp. 585-607, (1980)
46. Johnson, W.S., "Fatigue Testing and Damage Development in Continuous Fiber Reinforced Metal Matrix Composites," *Metal Matrix Composites: Testing, Analysis, and Failure Modes*, W. S. Johnson, Editor., ASTM STP 1032, pp. 194-221, Philadelphia, PA (1989)
47. Curtis, P.T. and Dorey, G., "Fatigue of Composite Materials," *Fatigue of Engineering Materials and Structures*, Vol II: Proceedings of the Institution of Mechanical Engineers, pp. 297-306, London (1986)
48. Hashin, Z. and Rotem, A., "A Fatigue Failure Criterion for Fiber Reinforced Materials," *Journal of Composite Materials* vol. **7**, pp. 448-464, (1973)
49. Radon, J.C. and Wachnicki, C.R., "Biaxial fatigue of glass fiber reinforced polyester resin," *Multiaxial Fatigue*, ASTM STP 853, K. J. Miller and M. W. Brown, Editors., ASTM, pp. 396-412, Philadelphia (1985)
50. Grimes, G.C., Ranger, K.W., and Brunner, M.D., "Element and Subcomponent Tests," *Composites*, T. J. Reinhart, Editor., pp. 313-345, Menlo Park, Ohio (1987)
51. Soemardi, T.P., Lai, D., and Bathias, C., "Static and Fatigue Biaxial Testing of Fiber Composites Using Thin Walled Tubular Specimens," *IUTAM Symposium*, Troy, N.Y. 1990, George J. Dvorak, Editor., Springer-Verlag, pp. 581-603, New York (1993)
52. Rosen, B.W. and Hashin, Z., "Analysis of Material Properties," *Composites*, T. J. Reinhart, Editor., ASM International, pp. 185-205, Metals Park, OHIO (1987)
53. Swanson, S.R., Christoforu, A.P., and Colvin, Jr., G.E., "Biaxial Testing of Fiber Composites Using Tubular Specimens," *Experimental Mechanics* vol. **28**, pp. 238-243, (1988)

54. Desalvo, G. J. and Gorman, R. W., *Ansys Engineering Analysis System; User's Manual*, Swanson Analysis System Inc., (1989)
55. Springer, G. S., *Environmental Effects on Composite Materials*, Technomic Publishing Co, Inc., (1981)
56. Gillat, O. and Broutman, L.J., *Advanced Composite Materials-Environmental Effects*, ASTM STP 658, J. R. Vinson, Editor., American Society for Testing and Materials, (1978)
57. Odom, E.M., Blackletter, D.M., and Suratno, B.R., "Experimental and Analytical Investigation of the Modified Wyoming Shear-test Fixture," *Experimental Mechanics* vol. **34(1)**, pp. 10-15, (1994)
58. Blackletter, D.M. and Odom, E.M., "Accurate and Precise Fabrication of Iosipescu Shear Test Specimens," *Journal of Testing and Evaluation* vol. **21(4)**, pp. 322-325, (1993)
59. Hull, D., *An Introduction to Composite Materials*, Cambridge University Press, Cambridge, U.K. (1988)
60. Purslow, D., "Some Fundamental Aspects of Composites Fractography", *Composites* vol. **12(4)**, pp. 241-247, (1981)
61. Purslow, D., "Matrix Fractography of Fibre-reinforced Epoxy Composites," *Composites* vol. **17(4)**, pp. 289-303, (1986)
62. Shin, E.S. and Pae, K.D., "Effects of Hydrostatic Pressure on In-Plane Shear Properties of Graphite/Epoxy Composites," *Journal of Composite Materials* vol. **26 (6)**, pp. 828-868, (1992)
63. Azzi, V.D. and Tsai, S.W., "Anisotropic Strength of Composites," *Experimental Mechanics* vol. **5**, pp. 283-288, (1965)
64. Kumosa, M. and Hull, D., "FEM Analysis of Mixed Mode Fracture in the Iosipescu Shear Test," *Sixth International Conference on Composite Materials; ICCM and ECCM II European Conference on Composite Materials*, F. L. Matthews, N. C. R. Bushell, J. M. Hodgkinson, and J. Morton, Editors., pp. 3.243-3.253, (1988)
65. Pindera, M.-J., Ifju, P., and Post, D., "Iosipescu Shear Characterization of Polymeric and Metal Matrix Composites," *Experimental Mechanics* vol. **30**, pp. 101-108,

(1990)

66. Kumosa, M. and Hull, D., "FEM Analysis of Mixed Mode Fracture in the Iosipescu Shear Test," *Sixth International Conference on Composite Materials / Second European Conference on Composite Materials*, F. L. Mathews, N. R. C. Buskell, J. M. Hodgkinson, and J. Morton, Editors., Elsevier Applied Science, pp. 3.243-3.253, (1987)
67. Barnes, J. A., *Torsion Testing of Filament Wound Composite Cylinders*, Ph.D. Thesis, University of Cambridge, Cambridge, U.K. (1986)

Vita

Balakrishnan was born on 2nd June 1967, in Trichy, Tamil Nadu, India. He received his Bachelors degree in Chemistry from St. Joseph's College, Trichy, India in 1987 and a Masters degree in Metallurgical Engineering from the Indian Institute of Science, Bangalore, India in 1991.